GEOLOGICA CARPATHICA, DECEMBER 2007, 58, 6, 511–530

Petrology, geochemistry and tectonic significance of Mesozoic ultramafic rocks from the Zagorje-Mid-Transdanubian Zone in Croatia

BOŠKO LUGOVIĆ[1], DAMIR SLOVENEC[2], JOSIP HALAMIĆ[2] and RAINER ALTHERR[3]

[1]Institute of Mineralogy, Petrology and Mineral Deposit, Faculty of Mining, Geology and Petroleum Engineering, University of Zagreb, Pierottijeva 6, HR-10000 Zagreb, Croatia; blugovic@rgn.hr
[2]Croatian Geological Survey, Sachsova 2, HR-10000 Zagreb, Croatia
[3]Mineralogisches Institut, Universität Heidelberg, Im Neuenheimer Feld 236, D-69120 Heidelberg, Germany

(Manuscript received June 13, 2006; accepted in revised form March 15, 2007)

Abstract: Ultramafic cumulates of Medvednica Mts form mega-blocks in the ophiolite mélange from the Zagorje-Mid-Transdanubian segment of the Sava Zone. The blocks consist of chromite-olivine cumulates and pyroxenites. The rocks crystallized in an open system under low pressure. Early crystallization of Al-Ti-chromite and Ti-edenite/pargasite indicate high oxygen fugacity hydrous parental magma. The Medvednica Mts ultramafic cumulates are analogous to plutonic rocks from recent immature island arcs. Subsolidus reactions indicate rapid exhumation with the final equilibration resembling prehnite-pumpellyite facies. The Medvednica Mts ultramafic cumulate sequence shows common features with the analogous sequence of the Bükk Mts ophiolites from NE Hungary and differ from analogues from the Vardar/Dinaric ophiolite belts. Mantle peridotites lacking overlying crustal members crop out in the Medvednica Mts and Kalnik Mts, and were cored in drill-holes. The peridotites range in composition from lherzolite via transitional harzburgite to depleted harzburgite. Lherzolite resembles abyssal peridotite and together with transitional harzburgites are akin to the peridotites from the South Sandwichs and Mariana arc–back-arc system. Depleted harzburgites are typical of fore-arc peridotites and are similar to the harzburgites of the Inner Dinaride Ophiolite Belt. Assuming that ultramafic rocks from the Zagorje-Mid-Transdanubian Zone were generated in a single oceanic domain, the South Sandwich arc-basin system appears as the most similar analogue. If it holds true, then these ultramafic rocks must have been derived from the Meliata-Maliac ocean domain and not from the Dinaric/Vardar strands as was previously thought.

Key words: Croatia, Zagorje-Mid-Transdanubian Zone, Medvednica Mts, geochemistry, petrology, ultramafic rocks, ophiolite mélange.

Introduction

Ultramafic cumulate rocks form the deepest sequence of the oceanic type crust and form the transitional zone to the mantle peridotites (e.g. Moores & Jackson 1974). Both units are integral parts of an ophiolite complex (e.g. Coleman 1977) and are often found in ophiolite mélanges worldwide. Such ultramafic rocks may make a crucial contributions to the interpretation of petrogenesis and geodynamic evolution of an ophiolite complex (e.g. Parlak et al. 1996, 2002; Huot & Maury 2002).

In the Sava Zone (SZ) segment of the Zagorje-Mid-Transdanubian Zone (ZMTDZ) fragments of ophiolite derived rocks are embedded along with blocks of various rocks of different geotectonic setting in chaotic sedimentary collages (ophiolite mélange) exposed at the SW tips of the ZMTDZ in the NW Croatia (Slovenec 2003, and references therein) and at the Bükk Mts in NE Hungary (e.g. Harangi et al. 1996; Aigner-Torres & Koller 1999; Faryad 2005). In general, both ophiolite mélanges contain scarce ultramafic cumulates and virtually lack mantle peridotites. Tectonic slices of mantle peridotites were found in the Medvednica Mts and Kalnik Mts and were drilled in a few oil-wells in the Sava Depression. Unlike in the ideal ophiolite pile (Anonymus 1972) and in many ophiolite complexes in the Dinarides (Robertson & Karamata 1994; Pamić et al. 2002, and references therein), these peridotite slices lack overlying ophiolite crustal members. This is the reason why the origin and relationship of these peridotites to the ultramafic cumulates, as well as to the other ophiolite members of the ophiolite mélange, are still obscure. Lugović & Slovenec (2004) have already attempted to research this problem.

The aim of this paper is to give overall characteristics of tectonite and cumulate ultramafic rocks from the SZ segment of the ZMTDZ with the intention of interpreting their genesis and working out the geotectonic setting of the formation, and finally, to correlate them with analogous rocks of ophiolite belts in the adjacent Dinarides.

Geological outlines

In the Dinarides ophiolites occur in two belts (Fig. 1A) with different characteristics (Nicolas & Jackson 1972; Pamić 1983; Smith & Spray 1984). The western belt,

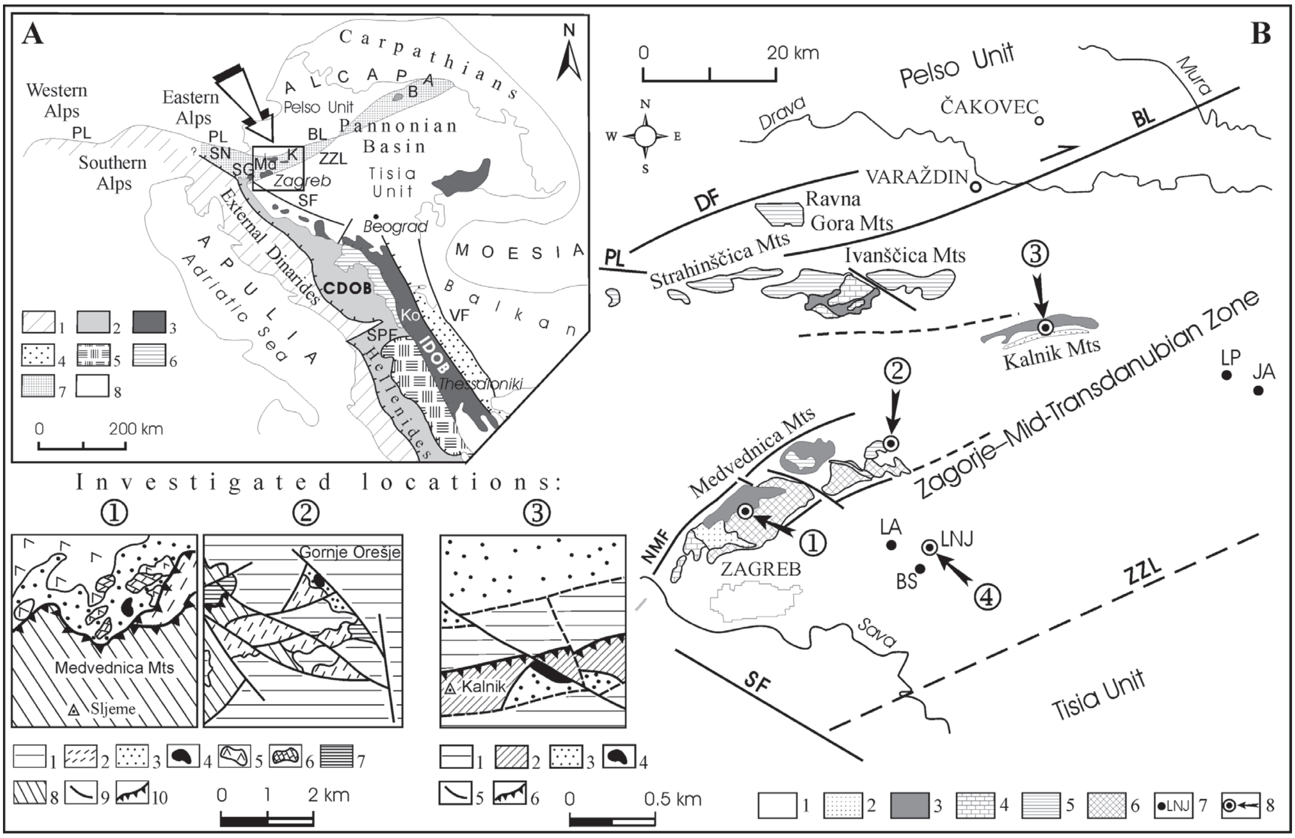

Fig. 1. A — Geotectonic sketch map of the Alps, Dinarides and Hellenides showing position of the Zagorje-Mid-Transdanubian Zone (ZMTDZ) (modified after Pamić 2002). **Legend:** 1 — External units, 2 — Central Dinaric Ophiolite Belt (CDOB) and Mirdita Zone, 3 — Periadriatic-Sava-Vardar Zone, including the Inner Dinaric Ophiolite Belt (IDOB), 4 — Serbo-Macedonian Massif, 5 — Pelagonides, 6 — Drina-Ivanjica element, 7 — Zagorje-Mid-Transdanubian Zone, 8 — Pannonian Basin. **Faults:** BL — Balaton Line, PL — Periadriatic Lineament, SF — Sava Fault, SN — Sava Nappe, SP — Skadar-Peć Fault, VF — Vardar Fault, ZZL — Zagreb-Zemplín Line. **Mountains:** B — Bükk Mts, I — Ivanščica, K — Kalnik, Ko — Kopaonik, Md — Medvednica, SG — Samoborska Gora. **B** — Geological sketch map of the ZMTDZ in Croatia (modified after Pamić & Tomljenović 1998). **Legend:** 1 — Neogene and Quaternary of the Pannonian Basin, 2 — Late Cretaceous-Paleocene flysch, 3 — Ophiolite mélange, 4 — Late Triassic platform carbonates, 5 — Late Paleozoic and Triassic clastics and carbonates interlayered with volcanics and tuffs, 6 — Lower Cretaceous metamorphic complex, 7 — deep oil-well penetrated ultramafic rocks (LA — Laktec, BS — Banje Selo, LNJ — Lonjica, LP — Lepavina, JA — Jagnjedovac), 8 — Site locations: 1 — Medvednica Mts, 2 — Gornje Orešje, 3 — Kalnik Mts, 4 — Sava Depression, oil wells. **Faults:** BL — Balaton Line, DF — Donački Fault, NMF — Northern Medvednica Fault, PL — Periadriatic Lineament, SF — Sava Fault, ZZL — Zagreb-Zemplín Line. **Insets** — Geological sketch maps of the sites 1 and 2 (modified after Pamić & Tomljenović 1998). **Legend:** 1 — Neogene and Quaternary sedimentary rocks, 2 — Late Cretaceous-Paleocene flysch, 3 — Ophiolite mélange with the mapable blocks of: 4 — ultramafics, 5 — mafics, 6 — limestones, 7 — Mesozoic, mostly Triassic clastics and carbonates, 8 — Lower Cretaceous metamorphic complex, 9 — normal faults, 10 — reverse or thrust faults. Geological sketch maps of the site 3 (modified after Šimunić et al. 1982). **Legend:** 1 — Neogene sedimentary rocks, 2 — Paleogene sedimentary rocks, 3 — Ophiolite mélange with ultramafic blocks (4), 5 — normal faults, 6 — reverse or thrust faults.

called the Central Dinaride Ophiolite Belt (CDOB), is dominated by mantle lherzolite (Lugović et al. 1991; Trubelja et al. 1995). The eastern belt, known as the Vardar Ophiolite Zone and corresponding to the Inner Dinaride Ophiolite Belt (IDOB, Smith & Spray 1984), is characterized by depleted mantle peridotites and has well developed igneous suites (Karamata et al. 1980). Its western segment stretches to the WNW and meets the CDOB in the SZ, whereas the eastern zone goes to the NE and continues to the Apuseni/Mures ophiolites in Romania (Karamata et al. 2000). Both ophiolite belts lay NW of the Scutari-Peć transform fault and are separated by the continental fragment called the Drina-Ivanjica element (Dimitrijević 1983; Robertson & Karamata 1994).

The ZMTDZ is located on the triple junction of the South Alpine Unit, Tisia block and the Internal Dinaridic Unit (Fig. 1A,B) and may correspond to the Gemer-Bükk subunit, located in the southern part of the Alcapa (Alpine-Carpathian-Pannonian) block of the Intra-Carpathian Area (ICA) (Harangi et al. 1996). The investigated realm is located at the SW termination of the ZMTDZ (Fig. 1A,B) and is composed of heterogeneous tectonostratigraphic units with ambiguously superimposed Dinaridic and Alpine structural elements (Herak 1999; Haas et al. 2000; Haas & Kovács 2001; Tomljenović 2002; Pamić 2003). The area is bounded by the north Croatian mountains, which include Medvednica, Kalnik, Ivanščica and Strahinjščica.

The Medvednica Mts are composed of a Lower Cretaceous basement consisting of very low- to low-grade metamorphic complex (Belak et al. 1995) in reversed-refolded thrust contact with the Middle Jurassic-Lower Cretaceous ophiolite mélange (Tomljenović 2002). These two units are the Medvednica Unit (MU) and Kalnik Unit (KU), respectively (Hass et al. 2000). The MU consists of metasedimentary successions of Silurian to early Carnian ages (Belak et al. 1995, and references therein), which are tectonically overlain by the Mesozoic metabasites (greenschists) of intraoceanic island arc provenance (Lugović et al. 2006). The KU contains fragments of different ophiolitic and sedimentary rocks ranging in age from Middle Triassic to Middle Jurassic (Halamić & Goričan 1995; Halamić 1998; Slovenec 1998; Halamić et al. 1998). The age of KU was palynologically dated as Middle Jurassic–Hauterivian (Babić et al. 2002). The ages of crystallization of ophiolitic extrusives from the KU are obscure since the whole-rock K-Ar measurements yielded Early to Middle Jurassic and Early to Late Cretaceous apparent ages (Pamić 1997) which are not consistent with the radiolarian ages of coherent chert-pillow basalt slices of late Ladinian–Carnian (Halamić & Goričan 1995; Goričan et al. 2005) and Jurassic ages (Halamić 1998; Halamić et al. 1999).

Cumulate ultramafites along with tectonite peridotites crop out only in the Medvednica Mts (Fig. 1B, sites 1 and 2). Ultramafic cumulate rocks form cm-dm to hm-km sized blocks (Kišpatić 1918; Crnković 1963; Šimunić et al. 1982) representing integral members of the KU (Fig. 1, inset 1). Some large blocks show the transition from ultramafic cumulate rocks to mafic cumulate and to isotropic gabbros (Crnković 1960; Slovenec 1998; Slovenec & Lugović 2000). The Medvednica Mts mantle peridotites were found near the village of Gornje Orešje in the form of two tectonic slices inserted within the Campanian-Maastrichtian rudist limestones (Šimunić & Pamić 1989) (Fig. 1, inset 2). The peridotites are transgressively overlain by sedimentary successions comprising Upper Cretaceous polymictic conglomerates and covered by Upper Badenian-Sarmatian conglomerates, limestones and marls. Peridotite exhumation must have happened before the Late Cretaceous as is inferred from the serpentinite infilling in rudist shells.

Tectonite peridotites were reported from the three localities in the Kalnik Mts (Fig. 1B, site 3) (Poljak 1942; Šimunić et al. 1981). Here, only one location was confirmed as a few meters large composite slice of serpentinized lherzolites underlain by amphibolites inserted in the upper Lower to Upper Cretaceous sedimentary succession (Fig. 1, inset 3). The amphibolites were interpreted as metamorphic sole (Šegvić et al. 2005).

Severely serpentinized mantle peridotites were cored in oil-wells in the ZMTDZ at Lonjica (LNJ), Laktec (LA) and Banje Selo (BS) (Fig. 1B, site 4) and SE from the Kalnik Mts at Lepavina (LP) and Jagnjedovac (JA) (Vragović & Marci 1973; Pandžić 1982). These peridotites are unconformably overlain by a Badenian sedimentary succession composed of conglomerates, sandstones and marls.

Analytical techniques

Mineral analyses from 10 representative samples were performed at the Mineralogisches Institut, Universität Heidelberg, using a CAMECA SX51 electron microprobe equipped with five wavelength-dispersive spectrometers. The operating parameters were 15 kV accelerating voltage, 20 nA beam current, ~1 μm beam size (10 μm for plagioclase) and 10 s counting time for all elements. Natural minerals, oxides (corundum, spinels, hematite and rutile) and silicates (albite, orthoclase, anorthite and wollastonite) were used for calibration. The raw data for all analyses were corrected for matrix effects with the PAP algorithm (Pouchou & Pichoir 1984, 1985) implemented by CAMECA. Formula calculations were done using a software package designed by Hans-Peter Meyer (Mineralogisches Institut, Universität Heidelberg).

Bulk-rock powders for chemical analyses of 10 samples were obtained from rock chips free of visible veins. Major elements and trace elements Rb, Ba, Sr, Zr, Cr and Ni were measured by wavelength dispersive XRF using conventional techniques. The trace elements: Cs, Th, U, Nb, Ta, Hf, Y and REE were analysed by ICP-MS at Actlab Laboratories in Toronto, Canada. Trace elements were determined from diluted solution after leaching 500 mg sample in 3 ml $HCl–HNO_3–H_2O$ at 95 °C for one hour and REE were analysed after $LiBO_2/Li_2B_4O_7$ fusion of 200 mg sample. Fe^{2+} was determined by manganometric titration in Zagreb. The H_2O was analysed by Karl-Fischer titration. The CO_2 contents were measured by infrared spectrometry after heating and combustion of the sample. H_2O and CO_2 were analysed in Karlsruhe.

Petrography

Ultramafic cumulates

Peridotite cumulates are poikilitic orthocumulates with chromite and olivine as ubiquitous cumulii crystals (Fig. 2A and 2B). Orthopyroxene, clinopyroxene and rare brown amphibole may also occur as cumulii. Early crystallized olivine and orthopyroxene cumulii are rounded and enclose opaque chromite. Intercumulus space is filled with up to 6 mm large postcumulus brown amphibole, clear clinopyroxene or orthopyroxene oikocrystals. All three intercumulus phases may be assembled in a single sample. In several samples calcic plagioclase ($An_{82–84}$) forms interstitial mesostasis. Igneous layering was not observed and neither mineral shows solid state deformation. Different modal proportion of cumulus and postcumulus phases allow us to distinquish the following peridotite cumulate types (Streckeisen 1974): amphibole lherzolite (P-6, Tables 1–6), plagioclase lherzolite (PB-1), amphibole harzburgite (MP-8, P-1) and plagioclase wehrlite (P-4).

Pyroxenite samples are either chromite-orthopyroxene-clinopyroxene adcumulates to mesocumulates (Fig. 2C) or chromite-olivine-orthopyroxene orthocumulate (Fig. 2D). Following the modal mineral classification and nomencla-

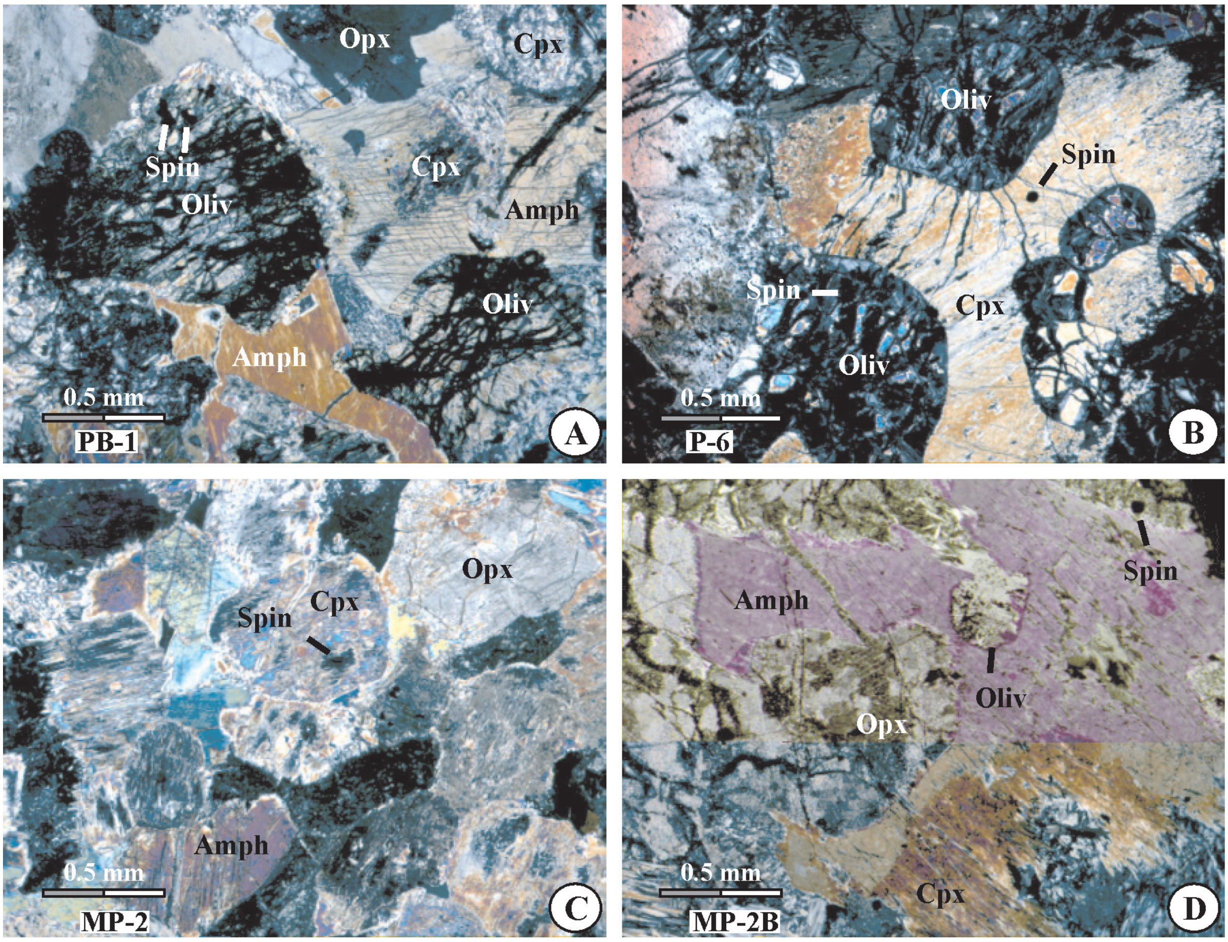

Fig. 2. A–D — Microphotographs of thin sections of ultramafic cumulates from the ZMTDZ taken with transmitted light and crossed polarizers. Abbreviations of mineral names are: Spin = spinel, Oliv = olivine, Opx = orthopyroxene, Cpx = clinopyroxene, Amph = amphibole. A — Sample PB-1, chromite-olivine-orthopyroxene-clinopyroxene orthocumulate (plagioclase lherzolite). The photo shows the domain where poikilitic amphibole fills intercumulus space. Other domains (not shown) contain clinopyroxene in intercumulus space. Chromite is enclosed in olivine relics floating in meshwork serpentine. B — Sample P-6, chromite-olivine orthocumulate with plagioclase mesostasis (plagioclase lherzolite). The photo shows a domain where poikilitic clinopyroxene fills intercumulus space. Other domains (not shown) contain amphibole or orthopyroxene as intercumulus infillings. Chromite occurs enclosed in olivine and as individual cumulii within the intercumulus. C — Sample MP-2, chromite-orthopyroxene-clinopyroxene adcumulate to mesocumulate (amphibole websterite). The photo shows adcumulate and mesocumulate domains of the sample. D — Sample MP-2B, chromite-olivine-orthopyroxeneorthocumulate (amphibole-olivine websterite). Large poikilitic amphibole and clinopyroxene fill the intercumulus space. Olivine is totally altered to serpentine-type mineral.

ture scheme of Streckeisen (1974), the analysed pyroxenites are represented by amphibole websterite (MP-2) and amphibole-olivine websterite (MP-2B). In the amphibole websterite, orthopyroxene and clinopyroxene are coalesced in adcumulate domains and the rest of the sample shows mesocumulate domains with interstitial brown amphibole. Amphibole-olivine websterite contains chromite, olivine and orthopyroxene as cumulus assemblage enclosed in large poikilitic brown amphibole and/or clinopyroxene.

Ultramafic cumulates show different alteration paragenesis. Relics of olivine are preserved only in peridotite cumulates. Olivine may be altered to or pseudomorphosed by the aggregate of chrysotile and magnetite, and occasionally of talk. Orthopyroxene is altered to lizardite along the cracks and chloritized at the grain periphery. Unlike in the cumulus peridotite, wherein clinopyroxene is slightly altered to actinolite and chlorite, in pyroxenites it occurs as relic in an aggregate consisting of various subsolidus Ca-amphiboles and cummingtonite. Plagioclase mesostasis in peridotite cumulate is soussiritized or replaced by the aggregate of prehnite and pumpellyite.

Tectonite peridotites

Tectonite peridotites are highly altered and their classification as lherzolite, transitional harzburgite and depleted harzburgite was inferred from the bulk-rock chemical composition and mineral chemistry of primary phases (see below).

Lherzolite. In the lherzolite sample (KC) brown-red spinel surrounded by ferrite-chromite is the only remaining primary mineral (Fig. 3A). Olivine is totally altered to serpentine. Orthopyroxene is replaced by bastite in the form of characteristic pseudomorphs indicating porphyroclastic texture. There are no virtual clinopyroxene pseudomorphs in the sample.

Transitional harzburgites. Transitional harzburgites (GO-1, GO-5 and GO-B) show porphyroclastic texture with the huge, ductile deformed orthopyroxene porphyroclasts set in the modest schistous matrix (Fig. 3B and 3C). The orthopyroxene porphyroclasts have thin lamellae (<3 μm) or granulae of exsolved clinopyroxene (Fig. 3C). Clinopyroxene occurs as small porphyroclast or individual grains in the matrix exsolving <4 μm wide lamellae (orthopyroxene?) totally altered to chlorite. In the samples GO-1 and GO-5, the matrix is composed of chrysotile/lizardite, magnetite and quartz with minor chlorite, talk, prehnite, and zeolite (Fig. 3B) whereas in the sample GO-B matrix also consists of relatively fresh, meshwork textured olivine, clinopyroxene (Fig. 3C) and minor calcic plagioclase ($An_{\sim 95}$). Ameboid opaque spinel is confined to the matrix as grains of variable size. Dolomite impregnations are abundant in the samples GO-5 and GO-B.

Depleted harzburgite. Although it shows comparatively the highest intensity of recrystallization, the depleted harzburgite (LNJ-1) is the least serpentinized sample (Fig. 3D). The sample has granuloblastic texture (Harte 1976) characterized by the clusters enriched in orthopyroxene and spinel with minor fresh olivine and accessory clinopyroxene surrounded by nearly pure, strongly serpentinized mosaic olivine. Primary amphibole fills the interstitial space of these clusters and may show a series of Ca-amphibole alterations. Spinel is idiomorphic rounded, dark brown to opaque, typical of hydrous peridotites.

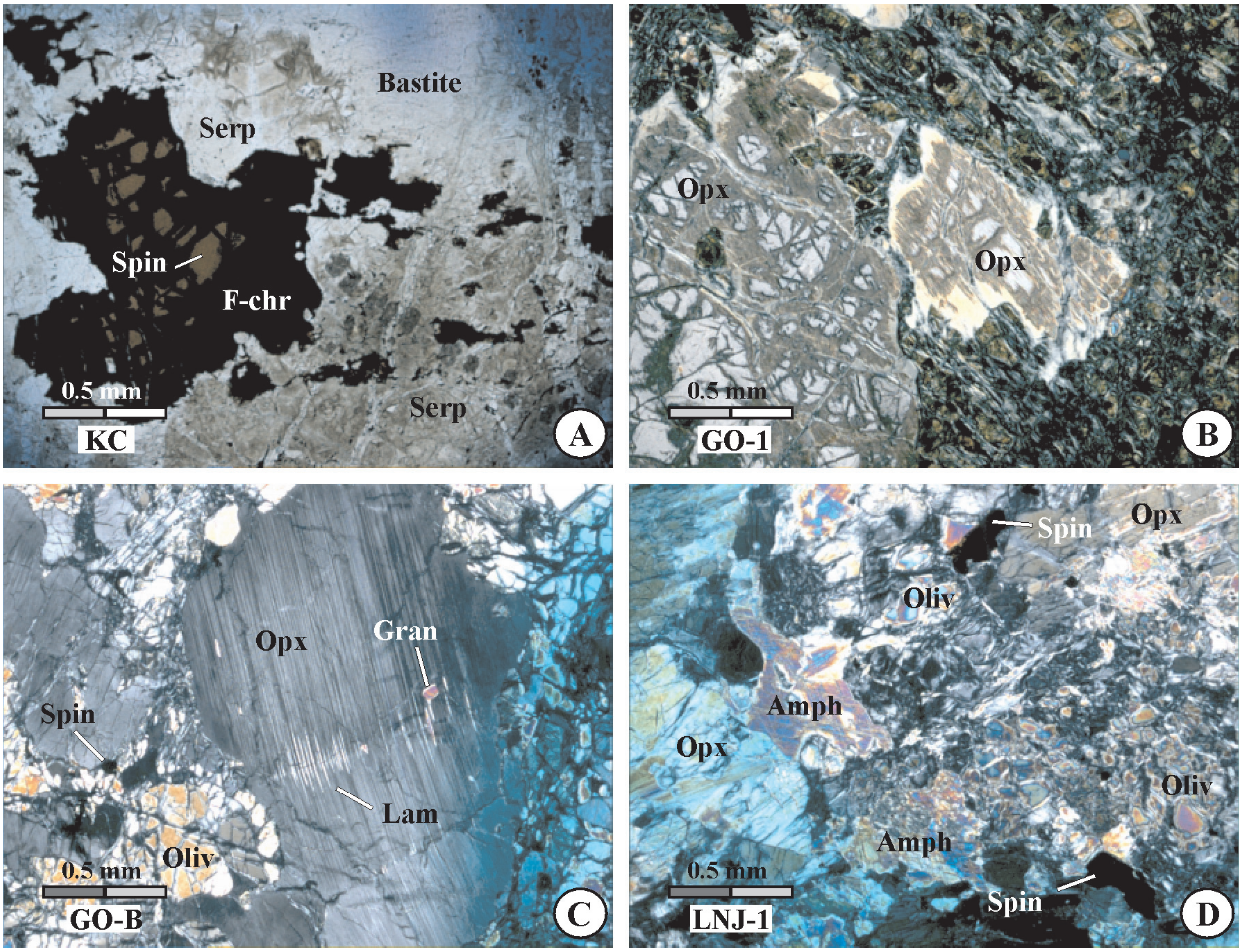

Fig. 3. A–D — Microphotographs of thin sections of tectonite peridotites from the ZMTDZ taken with transmitted light and crossed polarizers. Lam = lamellae, Gran = granulae; other abbreviations are as in Fig. 2. A — Sample KC, serpentinized lherzolite. Relic of ameboid to holly-leaf spinel in ferrit-chromite. Olivine is totally serpentinized and orthopyroxene bastitized. B — Sample GO-1, transitional harzburgite. Partly serpentinized and bastitized orthopyroxene porphyroclasts in the matrix of serpentinized olivine and minor relic clinopyroxene. C — Sample GO-B, plagioclase-bearing transitional harzburgite. Ductile deformed orthopyroxene porphyroclast in fresh matrix composed of olivine, clinopyroxene and spinel. Note clinopyroxene exsolution lamellae and granulae in orthopyroxene. D — Sample LNJ-1, amphibole-bearing depleted harzburgite. Amphibole is interstitial to orthopyroxene and olivine.

Mineral chemistry

Ultramafic cumulates

Selected chemical compositions of primary and some secondary phases from the analysed ultramafic cumulates are given in the Tables 1–5.

Spinel. Cumulii spinel is chromite. Chromite shows a narrow range of Cr# (0.506–0.644) and wide variation of Mg# (0.067–0.381) (Table 1; Fig. 4A). The spinels are significantly oxydized with Fe^{3+}# ranging from 0.170 to 0.480. TiO_2 content is generally high (> 1.17 wt. %). Chromite cumulii embayed in amphibole oikocrystal in amphibole harzburgite (MP-8) has the highest TiO_2 (6.5–7.0 wt. %), shows the lowest Mg# values (0.674–0.139) and the highest Fe^{3+}# (0.461–0.480). The NiO content of chromite ranges from 0.16 to 0.33 wt. %.

Olivine. Olivine shows a narrow compositional range with Mg# = 78.7–82.6 (Table 2). NiO content is typical of cumulus olivine (0.23–0.33 wt. %) and is positively correlated to Mg# (Fig. 4B). CaO is atypically low (0.02–0.15 wt. %).

Orthopyroxene. Orthopyroxene is enstatite ($Wo_{2.5-3.7}En_{78.4-81.5}Fs_{15.5-18.4}$) showing Mg# between 81.3 and 84.1 (Table 3; nomenclature after Morimoto 1988). The content of Al_2O_3 is low (1.39–1.95 wt. %). Rare orthopyroxene cumulii with low CaO ($Wo_{<1.1}$) contain significantly lower Al_2O_3 and Cr_2O_3 than coexisting intercumulus orthopyroxene (Fig. 4C).

Clinopyroxene. Clinopyroxene oikocrystals show compositional variation $Wo_{40.1-46.1}En_{46.3-49.9}Fs_{7.3-10.0}$ (Table 4) typical of magnesian augite to magnesian diopside (Morimoto 1988). Their Mg# (83.2–86.6) is higher than in coexisting orthopyroxene. Al_2O_3 is relatively low (2.07–2.95 wt. %; Fig. 4D) and Al^{VI}/Al^{IV} ratio is also low (<0.46). The content of Na_2O ranges from 0.21 to 0.43 wt. % and of Cr_2O_3 from 0.25 to 0.89 wt. %. TiO_2 ranges from 0.30 to 0.76 wt. %.

Amphibole. Amphibole oikocrystals have Mg# from 75.7 to 80.8 (Table 5) and correspond to pargasite and edenite (Fig. 5). In most samples amphibole oikocrystals contain appreciable Na_2O and Al_2O_3 (2.01–2.44 wt. % and 9.80–12.01 wt. %, respectively), variable TiO_2, and low Cr_2O_3 and K_2O (0.43–1.55 wt. %, 0.12–0.78 wt. % and

Table 1: Selected microprobe analyses and formulae of spinel from the Mesozoic ultramafic rocks of ZMDTZ.

	Ultramafic cumulates						Tectonite peridotites						
Site	①	①	①		①	①	③	②			②	②	④
Sample	P6	PB-1	MP-8	MP-8	MP-2	MP-2B	KC	GO-1	GO-1	GO-1	GO-5	GO-B	LNJ-1
Rock type	a-lhz	p-lhz	a-hzb		a-wbs	a-owbs	lhz	t-hzb			t-hzb	p-t-hzb	a-d-hzb
Anal. No.	17	8	5	6	13	6	6	1	2	35	17	3-2	5
Position	i,cpx	i,oliv	i,am	i,am	i,am	i,am	relic,c	lg,c	lg,r	mtx,c	mtx,c	sg,c	mtx
SiO_2	0.02	0.00	0.00	0.05	0.01	0.00	0.00	0.00	0.68	0.03	0.00	0.02	0.00
TiO_2	1.17	4.85	6.94	6.46	3.10	3.20	0.13	0.13	0.15	0.15	0.13	0.11	0.17
Al_2O_3	16.22	9.87	8.32	8.54	10.47	15.27	50.35	31.61	31.61	31.71	29.93	32.95	20.11
Cr_2O_3	35.88	26.62	17.48	18.57	23.61	29.24	17.90	35.82	34.31	35.16	36.90	34.52	46.62
Fe_2O_3	14.73	22.90	28.83	28.09	28.50	17.38	1.29	2.60	2.35	2.82	2.58	2.70	2.84
FeO	23.78	30.33	33.91	35.66	28.56	28.41	10.95	14.99	14.81	15.75	17.40	13.64	18.69
MnO	0.27	0.28	0.34	0.57	0.34	0.33	0.15	0.18	0.15	0.07	0.13	0.12	0.13
NiO	0.23	0.22	0.30	0.31	0.27	0.19	n.a.	n.a.	n.a.	n.a.	0.16	n.a.	n.a.
MgO	7.17	4.34	2.82	1.45	4.38	5.15	18.86	14.26	14.86	13.88	12.47	15.28	10.63
CaO	0.08	0.00	0.02	0.04	0.00	0.03	0.03	0.00	0.00	0.00	0.00	0.00	0.02
Total	99.54	99.41	98.95	99.73	99.26	99.20	99.65	99.60	98.90	99.55	99.70	99.33	99.21
Si	0.000	0.000	0.000	0.002	0.000	0.000	0.000	0.000	0.020	0.001	0.000	0.001	0.000
Ti	0.029	0.127	0.187	0.174	0.082	0.081	0.003	0.003	0.003	0.003	0.003	0.002	0.004
Al	0.634	0.407	0.352	0.361	0.432	0.610	1.590	1.100	1.100	1.106	1.059	1.136	0.753
Cr	0.940	0.736	0.496	0.527	0.653	0.784	0.379	0.836	0.801	0.823	0.876	0.798	1.171
Fe^{3+}	0.367	0.602	0.778	0.759	0.751	0.443	0.026	0.058	0.052	0.063	0.058	0.059	0.068
Fe^{2+}	0.659	0.887	1.017	1.071	0.836	0.805	0.245	0.370	0.366	0.390	0.437	0.334	0.497
Mn	0.008	0.008	0.010	0.017	0.010	0.009	0.003	0.005	0.004	0.002	0.003	0.003	0.004
Ni	0.006	0.006	0.009	0.009	0.008	0.005	-	-	-	-	0.004	-	-
Mg	0.354	0.226	0.151	0.077	0.229	0.260	0.753	0.628	0.654	0.612	0.559	0.666	0.503
Ca	0.003	0.000	0.001	0.002	0.000	0.001	0.001	0.000	0.000	0.000	0.000	0.000	0.001
Mg#	0.349	0.203	0.129	0.067	0.215	0.244	0.754	0.629	0.641	0.611	0.561	0.666	0.503
Cr#	0.597	0.644	0.585	0.593	0.602	0.562	0.193	0.432	0.421	0.427	0.453	0.413	0.609
Fe^{3+}#	0.189	0.345	0.479	0.461	0.409	0.241	0.013	0.029	0.027	0.032	0.029	0.030	0.034

Site number refers to the Fig. 1B. lhz = lherzolite, hzb = harzburgite, wbs = websterite, owbs = olivine websterite, t-hzb = transitional harzburgite, d-hzb = depleted harzburgite; a-, p- = amphibole or plagioclase bearing assemblage. i = inclusion in clinopyroxene (cpx) and amphibole (am) intercumulus, and in olivine (oliv) cumulii, lg = large grain, mtx = matrix, sg = small grain, c = core, r = rim. Formulae calculated on the basis of 4 oxygens and 3 cations; Mg# = Mg/(Mg+Fe^{2+}), Cr# = Cr/(Cr+Al), Fe^{3+}# = Fe^{3+}/(Cr+Al+Fe^{3+}).

Table 2: Selected microprobe analyses and formulae of olivine from the Mesozoic ultramafic rocks of ZMTDZ.

	Ultramafic cumulates				Tectonite peridotites				
Site	①		①	①	②			④	
Sample	P-6	P-6	PB-1	MP-8	GO-B	GO-B	GO-B	LNJ-1	LNJ-1
Rock type	a-lhz		p-lhz	a-hzb	p-t-hzb			a-d-hzb	
Anal. No.	19	20	10	31	3-1	5-6	5-8	39	41
Position	cum,c	cum,r	cum,c	cum,c	i,spin	spcl,r	spcl,c	spcl,r	spcl,c
SiO_2	39.25	39.11	39.18	38.60	40.63	41.09	40.74	41.09	40.94
TiO_2	0.02	0.03	0.00	0.01	0.00	0.00	0.02	0.01	0.01
Al_2O_3	0.01	0.02	0.01	0.01	0.03	0.01	0.00	0.03	0.00
Cr_2O_3	0.03	0.00	0.02	0.00	0.07	0.01	0.04	0.01	0.02
FeO	16.37	16.82	7.74	19.62	8.02	9.20	9.25	7.15	6.96
MnO	0.31	0.24	0.22	0.25	0.13	0.17	0.25	0.15	0.15
NiO	0.27	0.33	0.26	0.31	0.43	0.37	0.41	0.35	0.34
MgO	43.45	43.13	43.37	40.67	50.16	48.48	48.24	51.20	50.85
CaO	0.08	0.07	0.06	0.05	0.03	0.04	0.03	0.01	0.02
Total	99.80	99.77	100.85	99.52	99.49	99.37	98.97	100.00	99.29
Si	0.996	0.995	0.990	0.998	0.995	1.011	1.007	0.996	0.999
Ti	0.000	0.001	0.000	0.000	0.000	0.000	0.000	0.000	0.000
Al	0.000	0.001	0.000	0.000	0.001	0.000	0.000	0.001	0.000
Cr	0.001	0.000	0.000	0.000	0.001	0.000	0.001	0.000	0.000
Fe^{2+}	0.347	0.358	0.375	0.424	0.164	0.189	0.191	0.145	0.142
Mn	0.007	0.005	0.005	0.005	0.003	0.004	0.005	0.003	0.003
Ni	0.005	0.007	0.005	0.007	0.008	0.007	0.008	0.007	0.007
Mg	1.644	1.636	1.633	1.567	1.831	1.777	1.778	1.850	1.849
Ca	0.002	0.002	0.002	0.002	0.001	0.001	0.001	0.000	0.000
Total	3.003	3.004	3.010	3.002	3.004	2.989	2.992	3.003	3.001
Mg#	82.6	82.0	81.3	78.7	91.8	90.4	90.3	92.7	92.9

Site number refers to the Fig. 1B. lhz = lherzolite, hzb = harzburgite, t-hzb = transitional harzburgite, d-hzb = depleted harzburgite; a-, p- = amphibole or plagioclase bearing assemblage. cum = cumulii, i = inclusion in spinel (spin), spcl = small porphyroclast, c = core, r = rim. Formulae calculated on the basis of 4 oxygens and all Fe as FeO; Mg# = 100*Mg/(Mg+Fe^{2+}).

0.05–0.24 wt. %, respectively). In the amphibole harzburgite (MP-8), intercumulus amphibole shows a distinct composition being comparatively the richest in Na_2O and TiO_2 (2.59–2.87 wt. % and 2.67–3.64 wt. %, respectively). Amphibole inclusions in intercumulus clinopyroxene in amfibole websterite (MP-2B) show composition intermediate between these two groups but are apparently rich in Cr_2O_3 (1.19–1.57 wt. %). Retrograde Ca-amphiboles after primary amphiboles show a range of compositions from magnesiohornblende to actinolite and tremolite (Fig. 5) and cummingtonite (Table 5).

Tectonite peridotites

Selected chemical composition of primary and some secondary phases from the analysed tectonite peridotites are given in the Tables 1–5.

Spinel. In terms of Mg# and Cr# spinel shows a discontinuous range of composition (Table 1; Fig. 4A) which is typical of all three groups of Alpine-type peridotites (Dick & Bullen 1984) and resembles the trend of increasing depletion going from the spinel peridotites of passive margins through mature oceans to subduction-related active margins (Bonatti & Michael 1989). Spinel from lherzolite (KC) has the most fertile compositions, whilst the spinel from depleted harzburgite (LNJ-1) displays the most depleted compositions. Spinel from the transitional harzburgites (GO-1, GO-5 and GO-B) shows intermediate compositions (Mg# = 0.561–0.666; Cr# = 0.309–0.471). The Fe^{3+} abundance of spinel is low (Fe^{3+}# <0.048) and systematic variation of Fe^{3+} with respect to the degree of depletion was not observed. The TiO_2 content is low (<0.25 wt. %) and tends to increase as spinel Mg# decreases. The NiO content is <0.19 wt. %.

Olivine. In transitional harzburgite (GO-B) olivine Mg# ranges from 89.9 to 92.1, NiO content varies from 0.34 to 0.45 wt. % and are typical of mantle peridotites (Table 2; Fig. 4B). There is positive correlation of NiO content with Mg# in these olivines at concentration range >0.40 wt. % NiO. Olivine from depleted harzburgite (LNJ-1) shows refractory composition with Mg# ranges from 92.7 to 93.5 and NiO content similar to the olivine from the transitional harzburgite (GO-B). The NiO content does not correlate with Mg# in the latter case. The CaO concentration is typically low (<0.07 wt. %).

Orthopyroxene. Orthopyroxene porphyroclasts and thin lamellae exsolved in clinopyroxene are enstatite with Mg# as high as of coexisting olivine (Table 3). The most depleted compositions are identical to the orthopyroxene compositions of IDOB harzburgites (Fig. 4C). Individual enstatite porphyroblasts from the transitional harzburgite (GO-1) show the highest compositional variation by up to 2 wt. % Al_2O_3 with maximum Al_2O_3 content measured in a lamella.

Clinopyroxene. Clinopyroxene is mostly chromian diopside, magnesian augite is rare (Table 4). Mg# ranges

Table 3: Selected microprobe analyses and formulae of orthopyroxene from the Mesozoic ultramafic rocks of ZMTDZ.

	Ultramafic cumulates					Tectonite peridotites										
Site	①		①			②					②		②		④	
Sample	P-6	P-6	MP-8	MP-8	MP-8	GO-1	GO-1	GO-1	GO-1	GO-1	GO-5	GO-5	GO-B	GO-B	LNJ-1	LNJ-1
Rock type	a-lhz		a-hzb			t-hzb					t-hzb		p-t-hzb		a-d-hzb	
Anal. No.	6	7	7	9	32	48	55	71	72	85	11	12	2-1	2-2	16	20
Position	i.cum	i.cum	cum	cum	cum	gr.exs	lam	pcl,c	pcl,r	pcl,c	pcl,c	pcl,r	pcl,j	pcl,r	pcl,j	pcl,r
SiO_2	55.06	55.17	54.93	54.18	55.33	53.65	53.25	55.01	55.32	54.02	55.48	55.47	55.96	56.04	57.01	57.84
TiO_2	0.24	0.30	0.29	0.20	0.18	0.06	0.04	0.08	0.04	0.06	0.03	0.07	0.03	0.05	0.07	0.05
Al_2O_3	1.71	1.59	1.39	1.95	0.80	5.48	6.06	2.82	2.82	4.44	3.03	3.07	2.69	2.48	1.32	1.12
Cr_2O_3	0.52	0.45	0.24	0.47	0.08	1.06	1.07	0.82	0.82	1.02	0.84	0.88	0.72	0.63	0.49	0.32
Fe_2O_3	1.28	2.05	0.79	1.04	0.77	0.71	1.02	1.06	0.44	1.30	0.87	0.82	0.00	0.63	0.43	0.00
FeO	10.04	9.35	11.19	10.90	11.38	5.78	5.73	5.33	5.55	5.26	5.06	5.41	6.18	5.39	4.53	4.68
MnO	0.20	0.25	0.28	0.30	0.31	0.17	0.15	0.11	0.08	0.21	0.14	0.12	0.13	0.16	0.18	0.15
MgO	29.88	30.67	29.67	29.03	30.17	31.99	31.74	33.03	32.93	32.45	33.25	33.22	32.97	33.66	35.24	35.24
CaO	1.90	1.40	1.23	1.54	0.55	0.97	0.96	1.19	1.44	1.04	1.34	1.24	1.33	1.15	0.53	0.57
Na_2O	0.03	0.04	0.00	0.01	0.03	0.00	0.00	0.00	0.00	0.00	0.04	0.01	0.00	0.01	0.01	0.01
Total	100.85	101.26	100.01	99.62	99.60	99.88	100.01	99.45	99.43	99.79	100.08	100.30	100.01	100.18	99.80	99.98
Si	1.935	1.927	1.949	1.933	1.968	1.862	1.847	1.915	1.924	1.876	1.916	1.914	1.936	1.932	1.960	1.980
Al	0.071	0.065	0.058	0.082	0.033	0.224	0.248	0.116	0.116	0.182	0.123	0.125	0.110	0.101	0.054	0.045
Ti	0.006	0.008	0.008	0.005	0.005	0.002	0.001	0.002	0.001	0.002	0.001	0.002	0.001	0.001	0.002	0.001
Cr	0.015	0.012	0.007	0.013	0.002	0.029	0.029	0.022	0.023	0.028	0.023	0.024	0.020	0.017	0.013	0.009
Fe^{3+}	0.034	0.054	0.021	0.028	0.021	0.019	0.027	0.028	0.011	0.034	0.023	0.021	0.000	0.016	0.011	0.000
Fe^{2+}	0.295	0.273	0.332	0.325	0.339	0.168	0.166	0.155	0.162	0.153	0.146	0.156	0.179	0.155	0.130	0.134
Mn	0.006	0.007	0.008	0.009	0.009	0.005	0.005	0.003	0.002	0.006	0.004	0.003	0.004	0.005	0.005	0.004
Mg	1.565	1.597	1.570	1.544	1.600	1.655	1.641	1.714	1.707	1.680	1.712	1.708	1.701	1.730	1.805	1.798
Ca	0.071	0.052	0.047	0.059	0.021	0.036	0.036	0.045	0.054	0.039	0.050	0.046	0.049	0.042	0.019	0.021
Na	0.002	0.003	0.000	0.001	0.002	0.000	0.000	0.000	0.000	0.000	0.003	0.001	0.000	0.000	0.000	0.001
Mg#	84.1	85.4	82.5	82.6	82.5	90.8	90.8	91.7	91.4	91.7	92.1	91.6	90.5	91.8	93.3	93.1
Wo	3.6	2.6	2.4	3.0	1.1	1.9	1.9	2.3	2.8	2.0	2.6	2.4	2.5	2.2	1.0	1.1
En	79.4	80.5	79.4	78.6	80.4	87.9	87.6	88.1	88.2	87.9	88.5	88.3	88.0	88.8	91.6	91.9
Fs	17.0	16.9	18.3	18.4	18.5	10.2	10.5	9.6	9.1	10.1	8.9	9.3	9.5	9.1	7.4	7.1

Site number refers to the Fig. 1B. lhz = lherzolite, hzb = harzburgite, t-hzb = transitional harzburgite, d-hzb = depleted harzburgite; a-, p- = amphibole or plagioclase bearing assemblage. i.cum = intercumulus, cum = cumulii, gr.exs = granulae exsolution in clinopyroxene, lam = lamellae in clinopyroxene, pcl = porphyroclast, c = core, r = rim. Formulae calculated on the basis of 6 oxygens and 4 cations. Mg# = $100*Mg/(Mg+Fe^{2+})$, Wo = $100*Ca/(Fe_{tot.}+Mn+Mg+Ca)$, En = $100*Mg/(Fe_{tot.}+Mn+Mg+Ca)$, Fs = $100*(Fe_{tot.}+Mn)/(Fe_{tot.}+Mn+Mg+Ca)$.

Table 4: Selected microprobe analyses and formulae of clinopyroxene from the Mesozoic ultramafic rocks of ZMTDZ.

	Ultramafic cumulates							Tectonite peridotites										
Site	①	①		①	①		②	②				②			②			④
Sample	P-6	PB-1	PB-1	MP-8	MP-2	MP-2	MP-2B	GO-1	GO-1	GO-1	GO-1	GO-5	GO-5	GO-5	GO-B	GO-B	GO-B	LNJ-1
Rock type	a-lhz	p-lhz		a-hzb	a-wbs		a-owbs	t-hzb				t-hzb			p-t-hzb			a-d-hzb
Anal. No.	24	14	24	17	9	10	4	22	53	63	68	4	24	36	2-3	2-4	5-5	33
Position	i.cum	i.cum	cum	i.cum	ad.gr,c	ad.gr,r	ad.gr,c	gr.exs	spcl,c	mtx	lam	lam	mtx	spcl,c	spcl,r	spcl,c	lam	spcl,c
SiO_2	53.03	51.64	51.50	51.48	52.55	51.86	52.14	51.04	50.57	51.91	52.05	51.95	52.44	51.53	52.19	51.70	51.96	54.44
TiO_2	0.23	0.34	0.30	0.74	0.56	0.58	0.67	0.21	0.16	0.14	0.16	0.12	0.09	0.14	0.12	0.13	0.12	0.09
Al_2O_3	1.71	3.08	2.56	2.81	2.15	2.70	2.67	5.06	6.00	3.79	3.85	3.89	3.31	4.09	3.40	4.12	3.61	1.50
Cr_2O_3	0.48	0.89	0.75	0.57	0.42	0.69	0.67	1.39	1.27	1.24	1.24	1.27	1.16	1.36	1.24	1.34	1.16	0.67
Fe_2O_3	0.94	1.12	2.74	1.55	0.87	1.75	1.37	0.37	0.48	0.19	1.38	1.10	0.21	1.61	0.68	0.06	0.74	0.08
FeO	3.69	4.85	3.64	4.11	4.19	4.10	4.16	2.33	3.17	2.41	1.65	1.47	2.21	1.25	1.92	2.73	1.79	1.78
MnO	0.07	0.15	0.17	0.25	0.15	0.14	0.11	0.10	0.14	0.10	0.06	0.03	0.11	0.07	0.11	0.08	0.10	0.10
MgO	16.44	16.97	17.64	16.13	16.36	16.49	16.55	16.66	18.18	16.87	19.33	17.03	17.29	17.04	17.73	16.48	16.85	17.55
CaO	22.67	20.10	19.74	21.16	22.41	21.51	21.47	22.28	19.17	22.75	20.08	23.12	22.68	22.83	21.98	22.60	23.24	23.58
Na_2O	0.33	0.23	0.28	0.43	0.24	0.29	0.36	0.12	0.08	0.10	0.11	0.16	0.13	0.17	0.16	0.17	0.12	0.39
Total	99.59	99.37	99.33	99.22	99.90	100.10	100.17	99.55	99.21	99.51	99.91	100.14	99.62	100.08	99.50	99.41	99.69	100.17
Si	1.948	1.903	1.897	1.904	1.929	1.902	1.908	1.864	1.844	1.897	1.881	1.886	1.912	1.873	1.902	1.893	1.896	1.969
Al^{IV}	0.052	0.097	0.103	0.096	0.071	0.098	0.092	0.136	0.156	0.103	0.119	0.114	0.088	0.127	0.098	0.107	0.104	0.031
Al^{VI}	0.022	0.037	0.009	0.026	0.022	0.019	0.023	0.082	0.102	0.061	0.045	0.052	0.054	0.048	0.048	0.071	0.052	0.033
Ti	0.006	0.009	0.008	0.020	0.015	0.016	0.018	0.006	0.004	0.004	0.004	0.003	0.002	0.004	0.003	0.004	0.003	0.002
Cr	0.014	0.026	0.022	0.017	0.012	0.020	0.019	0.040	0.037	0.036	0.035	0.037	0.033	0.039	0.036	0.039	0.033	0.019
Fe^{3+}	0.026	0.031	0.076	0.043	0.024	0.048	0.038	0.010	0.013	0.005	0.038	0.030	0.006	0.044	0.019	0.002	0.020	0.002
Fe^{2+}	0.113	0.150	0.112	0.127	0.129	0.126	0.127	0.071	0.097	0.074	0.050	0.045	0.067	0.038	0.059	0.083	0.055	0.054
Mn	0.002	0.005	0.005	0.008	0.005	0.004	0.003	0.003	0.004	0.003	0.002	0.001	0.003	0.002	0.003	0.003	0.003	0.003
Mg	0.900	0.932	0.968	0.889	0.895	0.902	0.903	0.907	0.988	0.919	1.041	0.922	0.939	0.923	0.963	0.900	0.917	0.946
Ca	0.892	0.794	0.779	0.838	0.881	0.845	0.842	0.872	0.749	0.891	0.777	0.899	0.886	0.889	0.858	0.887	0.909	0.914
Na	0.023	0.016	0.020	0.031	0.017	0.021	0.026	0.008	0.005	0.007	0.008	0.011	0.009	0.012	0.011	0.012	0.008	0.027
Mg#	88.8	86.2	89.6	87.5	87.4	87.8	87.7	92.7	91.1	92.6	95.4	95.4	93.3	96.1	94.3	91.5	94.4	94.6
Wo	46.1	41.5	40.1	44.0	45.6	43.9	44.0	46.8	40.5	47.1	40.7	47.4	46.6	46.9	45.1	47.3	47.7	47.6
En	46.5	48.8	49.9	46.7	46.3	46.8	47.2	48.7	53.4	48.6	54.6	48.6	49.4	48.7	50.6	48.0	48.1	49.3
Fs	7.3	9.7	10.0	9.3	8.1	9.3	8.8	4.5	6.2	4.3	4.7	4.0	4.0	4.4	4.2	4.7	4.1	3.1

Site number refers to the Fig. 1B. lhz = lherzolite, hzb = harzburgite, wbs = websterite, owbs = olivine websterite, t-hzb = transitional harzburgite, d-hzb = depleted harzburgite; a-, p- = amphibole or plagioclase bearing assemblage. i.cum = intercumulus, cum = cumulii, ad.gr = adcumulus grain, gr.exs = granulae exsolution in orthopyroxene, spcl = small porphyroclast, mtx = matrix, lam = lamellae in orthopyroxene, c = core, r = rim. Formulae calculated on the basis of 6 oxygens and 4 cations. Mg#, Wo, En and Fs as in Table 3.

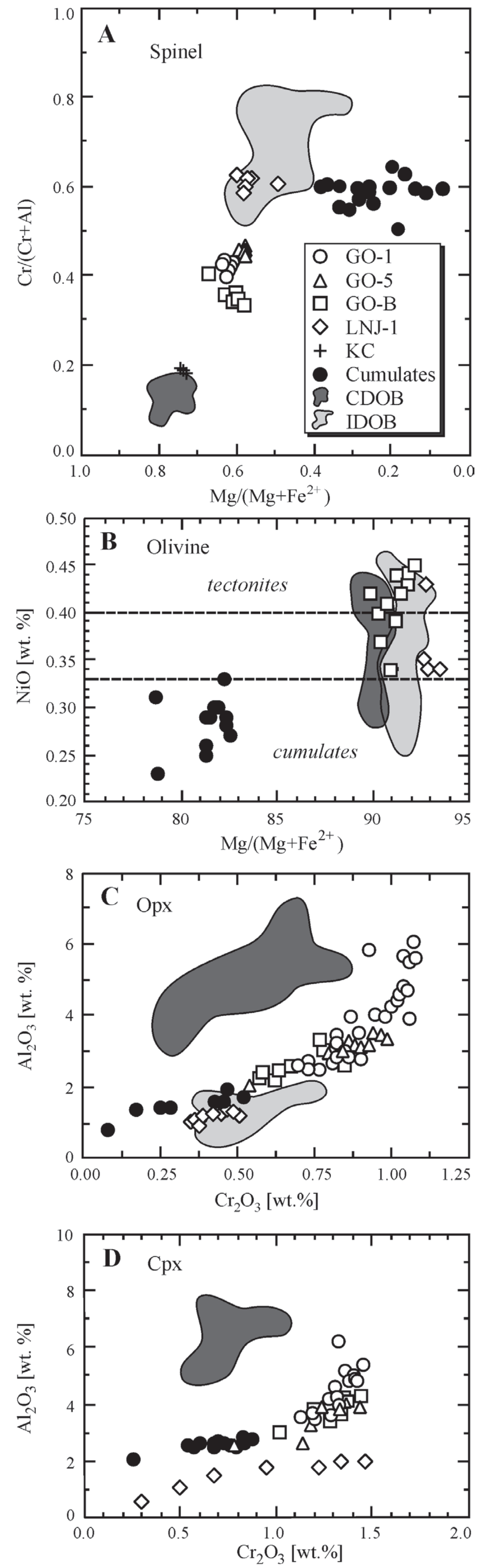

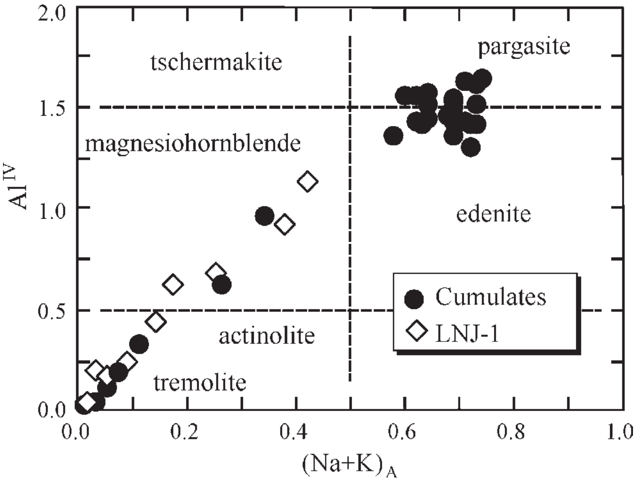

Fig. 5. Al^{IV} versus $(Na+K)_A$ classification diagram for amphiboles (Leake et al. 1997) from studied cumulus rocks (full circles) and depleted harzburgite, sample LNJ-1 (open circles). Primary amphiboles from the ZMTDZ ultramafic cumulates cluster in the fields of pargasite and edenite. The interstitial amphibole in depleted harzburgite LNJ-1 is magnesiohornblende.

from 90.0 in transitional harzburgites (GO-1, GO-5 and GO-B) to 96.2 in depleted harzburgite (LNJ-1) and is higher than in coexisting olivine and enstatite. Positive correlation between Al_2O_3 and Cr_2O_3 exists only in the clinopyroxenes from transitional harzburgites (Fig. 4D). Clinopyroxene is slightly more aluminian and significantly more chromian than coexisting enstatite. The Na content is low with <0.18 wt. % in the transitional harzburgites and <0.50 wt. % Na_2O in the depleted harzburgite. The TiO_2 content does not exceed 0.21 wt. %. Exsolved clinopyroxene, either lamellae or granulae, shows compositions similar to matrix clinopyroxene (samples GO-1 and GO-5).

Amphibole. Intestitial amphibole in depleted harzburgite (LNJ-1) corresponds to magnesiohornblende (Fig. 5) and shows a significant compositional variation accross the grains (Table 5). Late stage low-temperature alterations after clinopyroxene have an actinolitic to tremolitic composition.

Fig. 4. A–D — Plot of composition of spinel, olivine, orthopyroxene and clinopyroxene from the studied ultramafic rocks from the ZMTDZ. The compositional fields for CDOB and IDOB tectonite peridotites contoured after the data of Maksimović & Majer (1981), Lugović (1986), Maksimović & Kolomejceva-Jovanović (1987) are shown for the comparison. A — Plot of Cr/(Cr+Al) vs. $Mg/(Mg+Fe^{2+})$ in the spinel from the studied ultramafic rocks. For the rock type see Table 1. B — Plot of NiO vs. $Mg/(Mg+Fe^{2+})$ in the olivines from the studied ultramafic rocks. The boundary lines of tectonite and cumulate fields are from Leblanc et al. (1984). Symbols as in Fig. 4A. C — Plot of Al_2O_3 vs. Cr_2O_3 in the orthopyroxene from the studied ultramafic rocks. Symbols are as in Fig. 4A. Note that the points with the highest Al_2O_3 (~6 wt. %) correspond to the lamellae exsolved in clinopyroxene. D — Plot of Al_2O_3 vs. Cr_2O_3 in the clinopyroxene from the studied ultramafic rocks. Symbols are as in Fig. 4A.

Table 5: Selected microprobe analyses and formulae of amphibole from the Mesozoic ultramafic rocks of ZMTDZ.

	Ultramafic cumulates										Tectonite peridotites		
Site	①		①		①	①			①		④		
Sample	P-6	P-6	PB-1	PB-1	MP-8	MP-2	MP-2	MP-2	MP-2B	MP-2B	LNJ-1	LNJ-1	LNJ-1
Rock type	a-lhz		p-lhz		a-hzb	a-wbs			a-owbs		a-d-hzb		
Anal. No.	32	37	1	31	16	3	7	15	2	7	17	28	29
Position	i.cum	alt,am	i.cum	alt,am	i.cum	i.cum	i.cum	sec	i.cum	i,cpx	alt,cpx	isg,j	isg,r
SiO_2	45.09	54.89	45.64	50.34	43.37	44.75	44.68	57.76	45.12	43.30	56.93	48.67	53.13
TiO_2	2.36	0.42	0.60	0.25	3.64	2.52	1.02	0.03	1.26	2.91	0.15	0.63	0.30
Al_2O_3	10.37	2.69	10.66	6.34	11.07	10.30	11.68	0.26	10.44	11.30	1.51	9.08	5.73
Cr_2O_3	0.37	0.60	0.64	0.19	0.19	0.16	0.24	0.00	0.39	1.57	0.18	1.86	1.27
Fe_2O_3	0.00	0.00	2.00	1.63	0.00	0.00	2.51	0.00	1.17	0.00	0.00	0.00	0.00
FeO	7.65	5.47	5.83	5.37	8.56	7.79	5.52	12.10	7.37	8.29	1.58	2.37	2.07
MnO	0.09	0.05	0.11	0.16	0.12	0.09	0.16	0.34	0.11	0.11	0.10	0.09	0.07
MgO	17.32	20.57	17.61	19.10	16.10	17.20	16.84	26.37	16.97	15.37	23.32	19.52	21.31
CaO	11.16	12.50	11.43	11.90	11.11	11.18	12.07	0.74	11.57	11.79	12.96	12.69	13.11
Na_2O	2.56	0.40	2.10	1.15	2.83	2.63	2.12	0.07	2.34	2.62	0.21	1.59	1.00
K_2O	0.19	0.06	0.20	0.09	0.10	0.20	0.12	0.01	0.20	0.14	0.03	0.02	0.00
H_2O	2.08	2.15	2.08	2.10	2.06	2.07	2.08	2.17	2.07	2.06	2.18	2.12	2.18
Total	99.24	99.80	98.90	98.62	99.16	98.89	99.04	99.85	99.02	99.46	99.13	98.64	100.17
Si	6.508	7.652	6.574	7.176	6.313	6.490	6.439	7.973	6.538	6.302	0.830	6.874	7.320
Al^{IV}	1.492	0.348	1.426	0.824	1.687	1.510	1.561	0.027	1.462	1.698	0.170	1.126	0.680
Al^{VI}	0.271	0.095	0.384	0.240	0.213	0.251	0.423	0.016	0.321	0.241	0.075	0.385	0.251
Ti	0.257	0.044	0.064	0.026	0.399	0.275	0.111	0.003	0.137	0.318	0.015	0.067	0.031
Cr	0.043	0.066	0.073	0.022	0.022	0.019	0.028	0.000	0.045	0.181	0.019	0.207	0.139
Fe^{3+}	0.000	0.000	0.217	0.175	0.000	0.000	0.272	0.000	0.128	0.000	0.000	0.000	0.000
Fe^{2+}	0.692	0.514	0.466	0.458	0.857	0.725	0.528	1.397	0.690	0.910	0.098	0.219	0.193
Mn	0.011	0.006	0.013	0.020	0.015	0.011	0.020	0.040	0.014	0.014	0.012	0.011	0.008
Mg	3.726	4.274	3.782	4.059	3.494	3.719	3.618	5.426	3.666	3.336	4.782	4.111	4.378
Fe^{2+}	0.231	0.123	0.236	0.182	0.185	0.220	0.137	-	0.204	0.099	0.084	0.061	0.045
Ca	1.726	1.867	1.764	1.818	1.733	1.737	1.863	0.110	1.796	1.839	1.909	1.919	1.936
Na	0.042	0.010	0.000	0.000	0.082	0.043	0.000	0.008	0.000	0.062	0.007	0.020	0.019
Na	0.673	0.099	0.587	0.318	0.717	0.696	0.593	0.010	0.657	0.676	0.048	0.416	0.247
K	0.034	0.010	0.036	0.017	0.018	0.037	0.022	0.002	0.037	0.025	0.005	0.003	0.000
Total	15.708	15.109	15.623	15.335	15.736	15.733	15.615	15.012	15.694	15.701	15.053	15.419	15.247
Mg#	80.1	87.0	84.3	86.4	77.0	79.7	84.5	79.5	80.4	76.8	96.3	93.6	94.8

Site number refers to the Fig. 1B. lhz = lherzolite, hzb = harzburgite, wbs = websterite, owbs = olivine websterite, d-hzb = depleted harzburgite; a-, p- = amphibole or plagioclase bearing assemblage. i.cum= intercumulus, sec = secodary amphibole, i = inclusion in clinopyroxene (cpx) adcumulus grain, alt = alteration after intercumulus amphibole (am) or clinopyroxene (cpx), isg = interstitial grain, c = core, r = rim. Formulae calculated on the basis of 23 oxygens and 15 cats excluding K, Na to fit the structural positions to T = 8.00, M1-3 = 5.00 and M4 = 2.00. Note different cation allocation in cummingtonite formula (MP-2; 15). H_2O corresponds to 2 (OH) per formular units. Mg# = 100*Mg/(Mg+Fe^{2+}).

Bulk-rock chemical composition

Ultramafic cumulates

The chemical composition of ultramafic cumulates is shown in Table 6. High volatile values (8–11 wt. %) point to severe alteration of ultramafic cumulate rocks. Mg# is high and varies from 75.1 to 81.4. The abundances of incompatible elements Rb, Ta, U, and Nb in a few samples are under the detection limits. The content of LILE (K, Na, Ba, Cs) varies inconsistently. Immobile HFSE (Ti, Zr, Hf, Y, P) and REE retain igneous ratios (Zr/Hf = 33.3–40.0, Sm/Nd = 5.7–20.7). Contents of Cr and V are high and there is no significant difference between their concentrations in peridotites and websterite as it holds true for Ni and Co. The contents of CaO (1.26–11.50 wt. %) and Al_2O_3 (2.43–5.23 wt. %) reflect variable abundance of modal augite and amphibole, as well as by intensity of alteration. TiO_2 content is lower than 0.24 wt. %.

In the spider diagram with element concentrations normalized to primitive mantle (Fig. 6), excluding Cs and occasionally Ba which are extremely concentrated by alteration processes, the contents of other elements correspond to primitive mantle values or are maximally twice as high. The normalized patterns show slight negative P and Ti anomalies. Amphibole harzburgite (MP-8), exceeding the Nb detection limit, shows negative Nb anomaly [$(Nb/La)_n = 0.75$].

Amphibole harzburgite (MP-8) has a flat REE pattern consistent with Na-enrichment in the intercumulus amphibole (Fig. 7). Amphibole websterite (MP-2) shows typical MORB-type REE patern. All other samples follow sim-

Table 6: Chemical composition of Mesozoic ultramafic rocks from the ZMTDZ.

	Ultramafic cumulates					Mantle peridotites				
Site	1	1	1	1	1	3	2	2	2	4
Sample	P-6	P-1	P-4	MP-8	MP-2	KC	GO-1	GO-5	GO-B	LNJ-1
Rock type	a-lhz	a-hzb	p-whr	a-hzb	a-wbs	lhz	t-hzb	t-hzb	p-t-hzb	a-d-hzb
SiO_2	37.34	36.11	32.96	39.22	40.82	38.20	43.23	39.50	43.50	46.22
TiO_2	0.13	0.13	0.16	0.24	0.14	0.05	0.03	0.03	0.04	0.11
Al_2O_3	4.34	4.08	2.43	5.23	3.82	2.25	1.96	1.93	1.53	1.45
Fe_2O_3	9.09	9.63	10.84	8.56	11.42	-	-	-	3.71	1.10
FeO	4.37	4.80	4.78	6.95	5.70	-	-	-	4.35	3.54
Fe_2O_{3total}	-	-	-	-	-	5.74	9.80	8.10	-	-
MnO	0.17	0.18	0.19	0.26	0.10	0.11	0.07	0.08	0.08	0.09
MgO	27.81	33.05	27.00	27.61	27.00	38.85	32.98	30.24	36.69	34.90
CaO	6.17	1.26	11.50	2.94	2.24	1.15	0.97	5.05	1.04	5.41
Na_2O	0.15	0.09	0.12	0.43	0.19	0.03	0.03	0.02	0.01	0.02
K_2O	0.03	0.03	0.03	0.01	0.01	0.01	0.02	0.01	0.01	0.04
P_2O_5	0.01	0.01	0.01	0.01	0.01	0.02	0.01	0.01	0.00	0.00
H_2O	10.64	10.65	10.24	8.58	8.35	n.a.	10.64	8.97	6.54	6.42
CO_2	0.06	0.19	0.09	0.51	0.48	n.a.	0.58	6.11	2.23	0.51
LOI	n.a.	n.a.	n.a.	n.a.	n.a.	13.92	n.a.	n.a.	n.a.	n.a.
Total	100.31	100.21	100.35	100.55	100.28	100.33	100.32	100.05	99.71	99.82
Mg#	79.8	81.4	76.8	77.1	75.1	93.1	87.0	88.1	89.5	93.2
Cs	3.0	3.2	2.8	4.1	0.8	<0.1	0.1	0.2	0.1	0.9
Rb	< 2	< 2	< 2	< 2	< 2	< 1	< 2	< 2	4	2
Ba	73	12	5	4	5	41	8	8	43	26
Th	0.12	0.14	0.09	0.15	0.07	< 0.05	< 0.05	< 0.05	< 0.05	0.08
U	< 0.01	< 0.01	< 0.01	< 0.01	< 0.01	0.52	< 0.01	0.11	0.04	0.03
Nb	0.2	< 0.2	< 0.2	0.7	< 0.2	0.8	< 0.2	< 0.2	< 0.2	< 0.02
Ta	< 0.01	< 0.01	< 0.01	< 0.01	< 0.01	< 0.01	< 0.01	< 0.01	0.03	0.01
Pb	< 5	< 5	< 5	< 5	< 5	12	< 5	< 5	< 5	61
Sr	19	8	7	11	8	42	86	335	43	13
Zr	14	8	11	20	10	2	4	6	3	4
Hf	0.4	0.2	0.3	0.5	0.3	0.5	< 0.1	0.1	< 0.1	0.1
Y	4.8	2.8	4.5	7.2	8.1	2.1	1.1	1.2	1.0	1.8
Cr	3590	4000	2910	2130	2250	3170	3240	4030	2570	>10.000
Ni	1800	1420	1710	1090	434	2010	1820	1190	1830	825
Co	102	119	125	93	63	152	116	106	109	n.a.
La	0.46	0.35	0.34	0.92	0.37	0.15	< 0.05	< 0.05	0.11	0.23
Ce	1.10	0.80	0.90	2.50	1.10	0.06	< 0.05	< 0.05	0.18	0.46
Pr	0.18	0.11	0.14	0.37	0.20	0.02	< 0.01	< 0.01	0.03	0.09
Nd	0.92	0.59	0.82	1.94	1.21	0.16	< 0.05	0.05	0.14	0.57
Sm	0.34	0.22	0.34	0.63	0.55	0.09	0.03	0.03	0.05	0.23
Eu	0.141	0.081	0.127	0.222	0.244	0.026	0.007	0.009	0.021	0.088
Gd	0.55	0.32	0.54	0.92	0.92	0.18	0.06	0.06	0.08	0.30
Tb	0.11	0.07	0.11	0.18	0.21	0.05	n.a.	n.a.	0.02	0.06
Dy	0.76	0.46	0.77	1.22	1.39	0.30	0.16	0.17	0.16	0.35
Ho	0.18	0.11	0.18	0.26	0.31	0.07	0.04	0.04	0.04	0.08
Er	0.60	0.35	0.57	0.88	1.00	0.22	n.a.	n.a.	0.14	0.22
Tm	0.085	0.050	0.080	0.128	0.138	0.038	0.025	0.025	0.025	0.037
Yb	0.53	0.35	0.54	0.80	0.85	0.25	0.19	0.18	0.18	0.25
Lu	0.093	0.062	0.088	0.127	0.134	0.039	0.031	0.030	0.032	0.036

Site number refers to the Fig. 1B. lhz = lherzolite, hzb = harzburgite, whr = wehrlite, wbs = websterite; t-hzb = transitional harzburgite, d-hzb = depleted harzburgite. a-, p- = amphibole or plagioclase bearing assemblage. Mg# = 100*MgO/(MgO + FeO_{total}), molar ratio. n.a. = not analysed. LOI = loss on ignition.

ilar MREE-HREE profile but are comparatively slightly LREE enriched. Their HREEs show normalized concentrations of 1.9 to 4.2 times ordinary chondrite but are not enriched [$(Tb/Yb)_{cn}$=0.88–1.09]. The analysed ultramafic cumulates may show slight negative Eu anomaly (Eu/Eu* =0.89–1.01).

Tectonite peridotites

The chemical composition of tectonite peridotites is shown in Table 6. The intensity of alteration ranges from moderate, in sample LNJ-1, to severe in all other samples and may include significant silicification and dolomitiza-

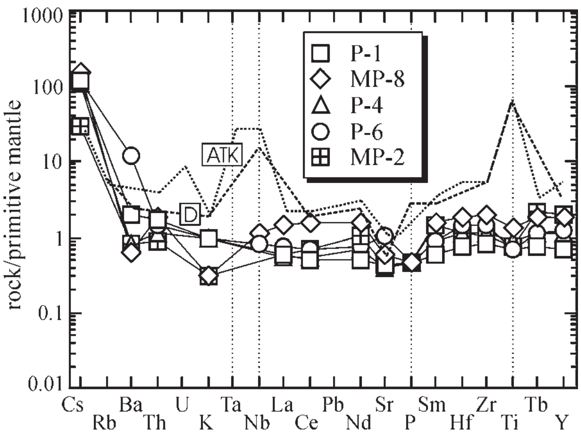

Fig. 6. Primitive mantle-normalized trace element concentration diagram for ultramafic cumulates from the ZMTDZ. Normalization values are from Hofmann (1988). For the rock type see Table 6. Cumulus peridotites (wehrlites) from the Bükk Mts (Downes et al. 1990; Aigner-Torres & Koller 1990) are shown for comparison. Note high positive Ta–Nb and Ti anomalies due to fractionation of Fe-Ti oxides in the latter.

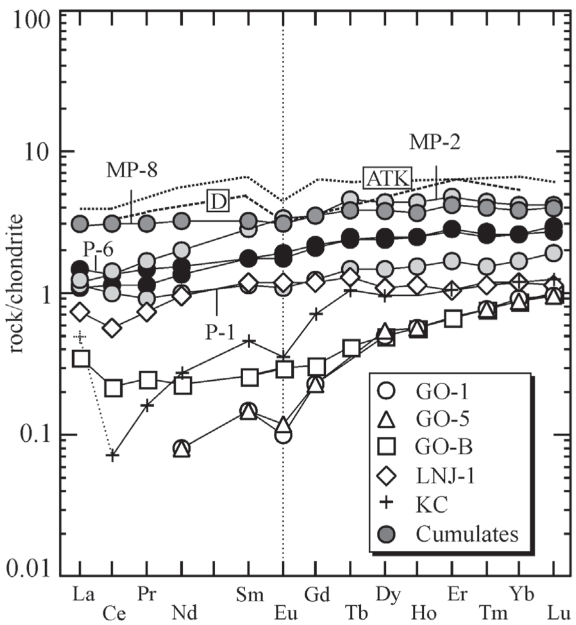

Fig. 7. Chondrite-normalized REE patterns of ultramafic rocks from the ZMTDZ. Normalizing values are from Evensen et al. (1978). For the rock type see Table 6; unlabelled full circle pattern represents plagioclase wehrlite, sample P-4. Wehrlites from the Bükk Mts (Downes et al. 1990; Aigner-Torres & Koller 1990) are shown as D and ATK, respectively. Note high negative Eu anomalies indicating a high fractionation level of Bükkian wehrlites.

tion. On account of normative clinopyroxene contents, the Al_2O_3 and CaO of bulk rocks (expressed on H_2O- and dolomite-free basis) peridotites from Gornje Orešje (Fig. 1B; site 2) are akin to transitional harzburgites (moderately depleted peridotites). For these harzburgites Mg# of 87.0 to 89.5 is apparently low suggesting significant loss of MgO during serpentinization. Serpentinized peridotite from the Kalnik Mts (Fig. 1B; site 3) reveals lherzolitic composition and peridotite from the drill-hole (Fig. 1B, site 4) resembles depleted harzburgite composition.

The primitive mantle normalized element abundance patterns reveal significant enrichment in LILE (Cs, Rb, Ba and Sr) in all samples, strong Pb spike in lherzolite (KC) and depleted harzburgite (LNJ-1), and the peaks of U, Hf and Zr in the lherzolite (not shown). These variations are inconsistent and most likely reflect polyphase alterations and, at least for Pb, also analytical uncertainly. We will not use these data for petrological and geochemical constraints.

The chondrite normalized REE patterns of tectonite peridotites are shown in Fig. 7. Lherzolite (KC) shows smooth LREE-depleted profile down to Ce and flat HREE profile. We assume that the shift of La concentration relative to Ce is an analytical error. Transitional harzburgites GO-1 and GO-5 show strongly depleted LREE profiles (La, Ce and Pr under detection limit) and MREE–HREE profiles have steep slopes ($Sm_{cn}/Lu_{cn} \approx 0.38$) within the range of 0.1 to 1 times chondrite content, typical of fertile to moderately depleted peridotites, respectively (Parkinson et al. 1992). These transitional harzburgites and the lherzolite show strong negative Eu anomaly ($Eu/Eu^* = 0.57$). Transitional harzburgite GO-B has a U-shaped REE pattern, whilst depleted harzburgite (LNJ-1) shows concave-up profile and neither show significant Eu anomalies.

Geothermometry

A summary of geothermometric estimations is given in Fig. 8.

In the *ultramafic cumulates,* high wollastonite in augite and low in the coexisting enstatite measured at a single contact, depict a low rate of subsolidus equilibrium. In the graphic geothermometer of Lindsley (1983) analysed pyroxenes yielded temperatures between 1100 °C and 900 °C. The equilibrium temperatures calculated for coexisting orthopyroxene and clinopyroxene for the geothermometers calibrated by Wells (1977) and Brey & Köhler (1990) are similar and range from 983 °C and 1029 °C depicting igneous temperatures. The temperatures calculated on the geothermometer Ca in enstatite (Brey & Köhler 1990) are significantly higher (1095 °C to 1191 °C) and, for the volatile saturated system appear too high. Coexisting pair of spinel *inclusions* in olivine yielded *rim-to-rim* temperatures between 860 °C and 790 °C (Fabriés 1979).

In *tectonite peridotites* two pyroxene geothermometer (Wells 1977) and olivine-spinel geothermometer (Fabriés 1979) gave the most consistent temperatures. The temperatures for coexisting orthopyroxene and clinopyroxene from transitional harzburgites GO-1 and GO-5 are 1021 ± 26 °C and 1004 ± 19 °C, respectively. The two pyroxene temperatures are significantly lower in plagioclase-bearing transitional harzburgite (GO-B) and depleted harzburgite (LNJ-1) (972 ± 17 °C and 883 ± 23 °C, respectively). In these peridotites temperatures for olivine-spinel

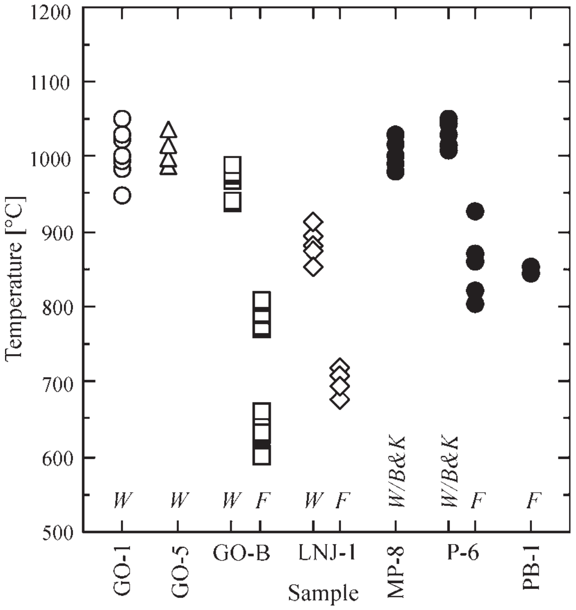

Fig. 8. Summary of geothermometric estimations for ultramafic rocks from the ZMTDZ. W and F refer to the temperatures calculated for coexisting orthopyroxene and clinopyroxene pairs, and for olivine and spinel pairs according to the thermometers calibrated by Wells (1977) and Fabriés (1979), respectively. W/B&K refers to the consistent orthopyroxene-clinopyroxene temperatures calculated after Wells (1977) and Brey & Köhler (1990). Rock symbols as in Fig. 7.

rim-to-rim pairs range from 810 °C to 600 °C and from 713 °C to 676 °C, respectively.

Discussion

Ultramafic cumulates

The textural patterns and mineral compositions of the Medvednica Mts ultramafic cumulates indicate that early chromite and olivine crystallized as cotectic minerals followed by enstatite, augite ± pargasite cumulii, postcumulus enstatite, augite, edenite/pargasite and finally by anorthite. Excluding spinel, the apparent homogeneous chemistry and narrow compositional range of primary minerals indicates an open crystallization system. Crystallization of Ti-pargasite in early phase of magmatic evolution suggests enhanced water content (>4 wt. %) in the parental magma (Koepke & Seidel 2004; Kocak et al. 2005). In the case of the Medvednica Mts ophiolitic rocks this is corroborated by igneous amphibole in mafic cumulates (Crnković 1960; Slovenec 1998). The cumulus and isotropic mafic-ultramafic rocks crystallized from volatile-rich magmas are almost exclusively found in subduction zones either in island arcs or continental margins (Conrad & Kay 1984; DeBari & Coleman 1989; Kocak et al. 2005). In the MORB setting, formation of Ti-pargasite is occasionally confirmed to the late-magmatic evolution of an intrusive sequence (Tribuzio et al. 2000).

The crystallization sequence of the Medvednica Mts cumulate rocks is typical of crystallization at low pressure. Relatively high Cr and low Al abundances and Al^{VI}/Al^{IV} ratio in augite (Table 4), as well as high Ti content in edenite/pargasite (Table 5) are evidence for low to moderate pressure fractionation of ultramafic cumulates related to arc region (compare to Hébert & Laurent 1990). Very low Ca in cumulus olivine (Table 2) points to subsolidus re-equilibration with enclosing amphibole and clinopyroxene. This also holds true for chromite cumulii embayed in amphibole oikocrystal in the amphibole harzburgite (MP-8) since they have the highest TiO_2 and Fe^{3+}# and show the lowest Mg# (Table 1). Cumulii spinel inclusions in olivine show a narrow range of Cr# and wide variation of Mg# (Table 1; Fig. 2A) which is typical of fast subsolidus Mg-Fe re-equilibration (Ozawa 1983) causing significantly lower blocking temperature compared to coexisting orthopyroxene-clinopyroxene pairs (Fig. 8).

The overall chemical composition of pyroxenes from the Medvednica Mts ultramafic cumulates and particularly low Al in orthopyroxene and low Ti in clinopyroxene are typical of pyroxenes assembled in the deepest intrusive sequences of magmatic arcs (Harris 1995) and forearcs (Ballantyne 1992). Chromite is found as one of the best petrologic and geotectonic indicators of the rocks (Kamenetsky et al. 2001) especially when it is, like in SZ ultramafic rocks, unique residual primary mineral. Medvednica Mts chromites are highly oxidized, show moderately high Cr# and relatively low Mg# (Table 1). In this respect they are similar to the plutonic spinels reported from magmatic arcs on continental margins (Kepezhinskas et al. 1993). The plutonic spinels from the Medvednica Mts have relatively high Ti abundance although the Ti contents of the bulk rock is low. This characteristic makes them essentially different from the fore-arc and back-arc intrusive spinels. Olivine from the Medvednica Mts ultramafic cumulates (Table 2) crystallized from the melt having Mg# 53–58 using olivine-melt K_d (= olivine/bulk rock FeO_{total}/MgO) of 0.30 (Roeder & Emslie 1970). Mafic island arc tholeiitic (IAT) extrusives from the Medvednica Mts ophiolite mélange have Mg# of 51–60 (Slovenec 1998) and their magma appears as a plausible source of olivine cumulii.

The geochemical affinity of the Medvednica Mts ultramafic cumulates was not well constrained due to the content of some diagnostic trace elements being under the detection limit. However, multi-element concentration normalized patterns of some analysed ultramafic cumulates show slight negative anomalies of HFS elements Ti, P and Nb (Fig. 6) typical for suprasubduction magmas, and the IAT magma affinity of these rocks is confirmed by their REE patterns (Fig. 7). In general, ultramafic cumulates from the ZMDT show similar normalized concentration patterns to cumulus wehrlites reported from the Bükk Mts. The essential difference is significantly higher level of fractionation in the latter case (Figs. 6 and 7), which caused extensive fractionation of Fe-Ti oxides — a typical characteristic of the North Hungarian ultramafic cumulates (Balla et al. 1983; Balla 1984; Kubovics 1984; Kubovics

& Bilik 1984; Downes et al. 1990; Harangi et al. 1996; Józsa 1999; Aigner-Torres & Koller 1999).

Tectonite peridotites

Although the mantle peridotites are severely serpentinized, the overall geochemical signatures allow them to be divided into three groups: (1) lherzolite from the Kalnik Mts (Fig. 1B, site 3), (2) transitional harzburgites from near Gornje Orešje in the Medvednica Mts (Fig. 1B, site 2), and (3) harzburgite from the Sava Depression (Fig. 1B, site 4). The spinel compositions clearly confirm the mantle origin of these peridotites and samples preserved coexisting olivine and spinel plot in the field of the olivine-spinel mantle array (OSMA) of Arai (1994) (Fig. 7).

The lherzolite from the Kalnik Mts (Table 6, sample KC) resembles the composition of fertile peridotite. Strong depletion in LREE relative to HREE (Fig. 7) suggests that residual lherzolite was formed after removal of very small increments of partial melts as was also concluded for CDOB (Central Dinaride Ophiolite Belt) lherzolites (Lugović et al. 1991). The low degree of partial melting of the lherzolite is corroborated by relatively fertile composition of relic spinel (Table 1). Assuming that entirely serpentinized olivine was coexisting with the relic spinel in the Kalnik Mts lherzolite the lercolite would represent the mantle residium after about 7 % partial melting (Fig. 7). The spinel composition (Table 1) is similar to the CDOB lherzolite spinel composition (Fig. 4A) and both spinels are consistent with the composition of spinels from pre-oceanic subcontinental and abyssal oceanic mantle peridotites as defined by Bonatti & Michael (1989).

The Medvednica Mts transitional harzburgites (Table 6, GO-1 and GO-5) are highly LREE depleted and show MREE-HREE profiles representative of depleted supra-subduction zone peridotites (Fig. 7). They are apparently akin to the depleted lherzolites and harzburgites from the recent (fore-arc) arc-basin systems such as the Mariana Trough (Parkinson & Pearce 1998), South Sandwich and, here, especially to the peridotites from the trench-fracture zone intersection (Pearce et al. 2000), and from ancient intra-oceanic arc settings such as that recorded by the South Ladakh ophiolites of the Indian Himalayas (Mahéo et al. 2004). The olivine-spinel composition suggests that the Medvednica transitional harzburgites represent mantle residium after approximately 20 % partial melting (Fig. 9). The Medvednica Mts plagioclase-bearing transitional harzburgite, sample GO-B (Table 6), shows LREE-MREE profile of the REE pattern which reflects the metasomatism of a peridotite similar to the transitional harzburgites represented by the samples GO-1 and GO-5 (Fig. 7). This transitional harzburgite recrystallized in the plagioclase-peridotite field as shown by their lower equilibration temperatures compared with unmetasomatized transitional harzburgites (Fig. 8). The spinel compositions from the Medvednica Mts transitional harzburgites indicate Type I peridotite host rocks (Dick & Bullen 1984), which are transitional between CDOB lherzolites and IDOB (Inner Dinaride Ophiolite Belt) harzburgites (Fig. 4A).

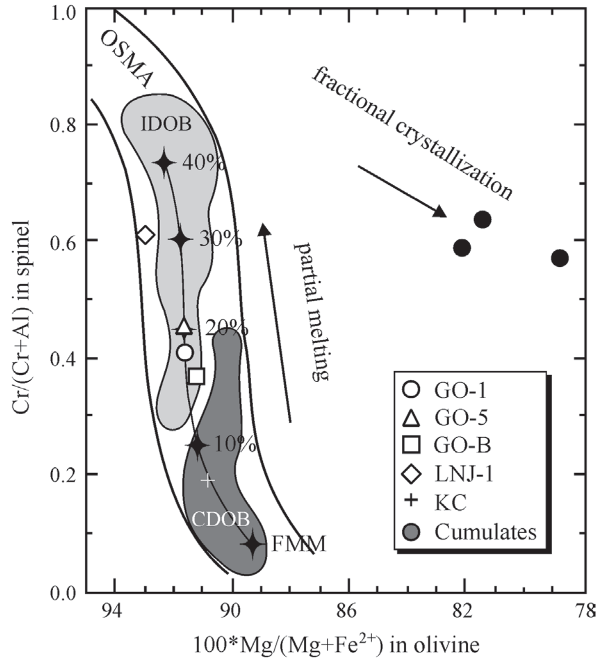

Fig. 9. Plot of Cr/(Cr+Al) in spinel against $100*Mg/(Mg+Fe^{2+})$ in olivine for ultramafic rocks from the ZMTDZ. The fields of spinels from the CDOB and IDOB peridotites contoured after data sources listed in Fig. 4. Olivine-spinel mantle array (OSMA) and partial melting trend annotated by % are from Arai (1994). FMM is fertile MORB mantle. Average spinels from tectonite peridotite samples KC, GO-1 and GO-5 were also plotted assuming their equilibration with olivine. Lherzolite from Kalnik Mts is akin to ocean ridge peridotites, whilst other analysed ZMTDZ peridotites, resemble oceanic supra-subduction zone (SSZ) peridotites. Ultramafic cumulates from the ZMTDZ form the poorly developed trend of fractional crystallization. CDOB peridotites plot in the fields of peridotites from passive margins and ocean ridges whilst IDOB peridotites occupy the field of oceanic SSZ peridotites.

The depleted harzburgite from the drill-hole in the Sava Depression (Table 6, sample LNJ-1) shows high Ca- and LREE-MREE-metasomatized signatures and in that respect may be misunderstood for least differentiated cumulus amphibole harzburgite (P-1) (Fig. 7). However, the spinel (Table 1) and olivine compositions (Table 2) of the sample indicate a mantle origin and suggest metasomatism after 30–33 % partial melting (Fig. 9). By composition these spinels are very similar to the spinels from the IDOB harzburgites (Fig. 4A). This sample showing the lowest equilibration temperatures (Fig. 8) suggests final equilibration in the plagioclase-peridotite facies. The Medvednica Mts ultramafic cumulates are most likely genetically related to the mantle peridotites represented by the LNJ-1 type lithology (Fig. 4).

The chemical compositions of coexisting spinel and orthopyroxene in terms of the Al_2O_3 in orthopyroxene and Cr/(Cr+Al) ratio in spinel were used to compare the peridotites of the Sava Zone with the peridotites from the CDOB and the IDOB. The analyses reported for spinel and orthopyroxene from active arc-basin systems, which appear to be the most liable recent analogues, were used as

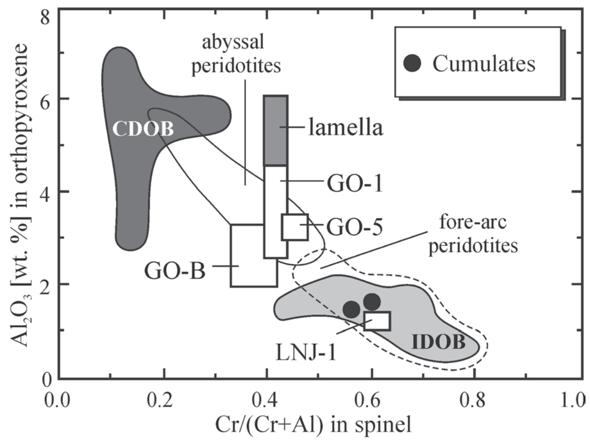

Fig. 10. Plot of Al_2O_3 content in orthopyroxene against Cr/(Cr+Al) in spinel for the tectonite peridotites and mafic cumulates from the ZMTDZ. Data source for CDOB and IDOB as in Fig. 4. The field of abyssal peridotites is given by Bonatti & Michael (1989) and the field for southern Mariana fore-arc peridotites comes from Ohara et al. (1996) and Ohara & Ishii (1998). Transitional harzburgites from the ZMTDZ plot in the field of abyssal peridotite of back-arc provenance whilst depleted harzburgite (LNJ-1) and IDOB peridotites plot in the field defined by fore-arc peridotites.

referent compositions. The relationship shown in Fig. 10 suggests that the mineral pairs were generated in the mantle similar to depleted abyssal peridotites (Bonatti & Michael 1989) and to analogues of recent arc-basin systems represented by the South Sandwichs (Pearce et al. 2000) or Mariana Trough (Ohara et al. 1996, 2002). Since the overall chemical compositions of Medvednica Mts transitional harzburgites are highly correlated with the recent back-arc peridotites from the South Sandwichs, we envisage a back-arc setting as the most plausible environment for these transitional harzburgites. The depleted harzburgite from the Sava Depression correlates to Mariana fore-arc peridotites (Ohara & Ishii 1998).

The CDOB peridotites (fertile lherzolites) are plotted beyond the field of abyssal peridotites and the IDOB peridotites (depleted harzburgites and dunites), repeatedly believed to have been formed in a back-arc setting (Robertson & Karamata 1994, and references therein) are stretched in the field of the fore-arc peridotites defined by the Mariana fore-arc peridotites.

The relationship of ultramafic cumulates to tectonite peridotites and the geotectonic implications

The block of ultramafic cumulate rocks from the Medvednica Mts ophiolite mélange is an integral part of the Kalnik Unit (Slovenec 1998; Haas et al. 2000) deposited from the Middle Jurassic to Hauterivian (Babić et al. 2002). The unit stretches further to the North, to the Ivanščica Mts, where an island-arc source was suggested for extrusive rocks from the Lower Cretaceous clastic deposits (Babić et al. 1979). The magmatic rocks found in the Kalnik Unit were constrained to the northwesternmost outcrops of the IDOB (Pamić 1997). The Kalnik Unit is presumed to stretch further to the NE in Hungary (Pamić & Tomljenović 1998) where an ophiolitic mélange crops out in the Mt Bükk (e.g. Balla et al. 1983). The origin in an arc to back-arc system was recognized for igneous rocks of this mélange (Balla 1984; Downes et al. 1990; Harangi et al. 1996; Aigner-Torres & Koller 1999).

The ultramafic cumulates from the Dinaric ophiolites crystallized from dry magmas and do not contain amphibole oikocrystals at all (Pamić 1974; Karamata 1979; Lugović 1986; Pamić & Desmons 1989; Majer 1993). These rocks seem not to be affected by Alpine regional low-grade metamorphism. Medvednica Mts ultramafic cumulates are thus more correlative to the ultramafic sequences of the Bükk Mts ophiolites which also contain abundant amphibole intercumulus and Ti-rich oxides (Balla et al. 1983; Balla 1984; Kubovics 1984; Kubovics & Bilik 1984; Downes et al. 1990; Harangi et al. 1996; Aigner-Torres & Koller 1999; Józsa 1999) and underwent similar prehnite-pumpellyite facies alterations during the Alpine orogeny (Árkai 1983).

The spinel compositions in the Berrriasian to Lower Albian clastic succession in the Gerecse Mts from the northern Transdanubian Mid-Mountains (Árgyelán 1996) suggest an origin from sources similar to the Medvednica Mts transitional harzburgite and ultramafic cumulates (Slovenec & Lugović 2000; Lugović & Slovenec 2004) and to depleted harzburgite from the Sava Depression. We explain this feature by the exposition of these types of peridotites to the weathering and accumulation of spinels in the sediments from this clastic succession. The spinel compositions of the Kalnik Mts lherzolite were not found in the Gerecse Mts clastic succession.

The variety of mantle peridotite composition revealed in only five samples from the Transdanubian segment of the Sava Zone suggest a diversity of tectonic settings of their formation. This is consistent with observations from elsewhere showing different tectonic settings for the ophiolite complexes within the same orogenic belt. Assuming that the mantle peridotites from the Transdanubian segment of the Sava Zone were generated in a single oceanic domain then they should resemble a fore-arc–arc–back-arc oceanic system. Similar relations may be inferred from the geochemical and petrological characteristics reported for ultramafic cumulates associated within the ophiolites from NW Hungary (Balla et al. 1983; Balla 1984; Kubovics 1984; Kubovics & Bilik 1984; Réti 1987; Downes et al. 1990; Harangi et al. 1996; Józsa 1999; Aigner-Torres & Koller 1999) and the diversity of mantle peridotites from the adjacent SW Slovakia (Hovorka et al. 1985).

The formation of MORB-type ocenic crust in the Transdanubian segment of the Sava Zone commenced in the late Ladinian (Halamić et al. 1998; Goričan et al. 2005). Ocean spreading may be traced till the Middle Jurassic (Halamić & Goričan 1995) when an accretionary wedge in front of the intra-oceanic arc was formed (Babić et al. 2002). The closure of this oceanic domain started around 120 Ma ago (Barremian–Aptian) by formation of a metamorphic sole (Šegvić et al. 2005) followed by obduction and greenschist facies metamorphism of the island arc onto the continental platform (Belak 1995; Lugović et al. 2006).

The CDOB metamorphic sole was dated by five five-points Sm-Nd isochrons to around 171 Ma (Olker et al. 2001) and between 172 and 159 Ma by K-Ar measurements on hornblende and white mica separates (Okrusch et al 1978). The emplacement of the Vardar ophiolites, namely the IDOB ophiolites, on the Pelagonian Continent was recorded by the ophiolitic detritus in the Middle to Upper Bathonian sediments, while ocean floor was still forming (Baumgartner et al. 1993).

Following all statements we consider the original oceanic domain where these ultramafic rocks were formed more akin to the Meliata-Maliac segment of the Tethys as defined by Stampfli & Borer (2002) (their Fig. 8) then to either Dinaric oceanic strand.

Conclusions

(1) The Medvednica Mts ultramafic cumulates consist of genetically related chromite-olivine ± opx ± cpx cumulates with abundant intercumulus edenite-pargasite. The rocks crystallized in a shallow open magma chamber from volatile-rich magmas favouring precipitation of Ti-rich spinel and amphibole.

(2) The ultramafic cumulates show a tholeiitic affinity typical of plutonic rocks from suprasubduction setting, most akin to fore-arc setting. They are genetically linked to depleted harzburgites from the Sava Depression.

(3) Subsolidus paragenesis shows a large temperature interval of alterations indicating fast exhumation of the ultramafic sequence. The most widespread alterations are of low-grade prehnite-pumpellyite facies.

(4) The Medvednica Mts ultramafic cumulate sequence shows different features than equivalent sequences in the CDOB and IDOB ophiolite complexes and correlates with the analogue from the Bükk Mts.

(5) The mantle peridotites resemble a diversity of tectonic settings typical of recent fore-arc–arc–back-arc oceanic systems. There is a correlative relationship to the tectonic setting of the Bükk Mts ophiolites in NW Hungary and to ophiolites in SW Slovakia.

(6) On the basis of the geochemical and petrogenetic signatures of analysed ultramafic rocks we locate the domain from which these rocks are derived in the Meliata-Maliac segment of the Tethys.

Acknowledgment: Financial support by the Croatian Ministry of Sciences, Technology and Sports to the ceased Projects Nos. 01959025, 0181001 and 0181006 is gratefully acknowledged. D.S. likes to acknowledge a current grant from the Ministry (Project 181-1951126-1141). Thanks are due to the charged people from INA-Naftaplin for easy access to relevant drill-cores. We thank I. Fin and H-P. Meyer from Mineralogisches Institut in Heidelberg for preparing polished thin sections and for providing excellent microprobe facilities, respectively. Constructive reviews by Friedrich Koller and Csaba Szabó helped to achieve the final version of this paper.

References

Aigner-Torres M. & Koller F. 1999: Nature of the magma source of the Szarvaskö complex (NE Hungary): petrological and geochemical constraints. *Ofioliti* 24, 1–12.

Anonymus 1972: Penrose field conference on ophiolites. *Geotimes* 17, 24–25.

Arai S. 1994: Characterization of spinel peridotites by olivine-spinel compositional relationships: Review and interpretation. *Chem. Geol.* 113, 191–204.

Árgyelán G.B. 1996: Geochemical investigations of detrital spinels as a tool to detect an ophiolitic source area (Gerecse Mountains, Hungary). *Acta Geol. Hung.* 39, 341–368.

Árkai P. 1983: Very low- and low- and low-grade regional metamorphism of the Paleozoic and Mesozopic formations of the Bükkium, NE-Hungary. *Acta Geol. Hung.* 26, 83–101.

Babić Lj., Zupanić J. & Crnjaković M. 1979: The recognition of the two units in the "clastic formation with ophiolites" of Mt. Ivanščica and the role of a magmatic belt and an active continental margin. *Zbornik radova, Znan. savj. naftu JAZU, Sekc. primj. geol., geofiz., geokem., 4. god. znanstv. skup*, 115–123.

Babić Lj., Hochuli A.P. & Zupanič J. 2002: The Jurassic ophiolitic mélange in the NE Dinarides: Dating, internal structure and geotectonic implications. *Eclogae Geol. Helv.* 95, 263–275.

Balla Z. 1984: The North Hungarian Mesozoic mafics and ultramafics. *Acta Geol. Hung.* 27, 341–357.

Balla Z., Hovorka D., Kuzmin M. & Vinogradov V. 1983: Mesozoic ophiolites of the Bükk Mountains (North Hungary). *Ofioliti* 8, 5–45.

Ballantyne P. 1992: Petrology and geochemistry of the plutonic rocks of the Halmahera ophiolite, eastern Indonesia, an analogue of modern oceanic forearcs. In: Parson L.M., Murton B.J. & Browning P. (Eds.): Ophiolites and their modern oceanic analogues. *Geol. Soc. Spec. Publ.* 60, 179–202.

Baumgartner P.O., Danelian T., Dumitrica P., Goričan S., Jud R., Dogherty L.O., Carter B., Conti M., De Wever P., Kito N., Marcucci M., Matsuoka A., Murchey B. & Urquart E. 1993: Middle Jurassic-Early Cretaceous radiolarian biochronology of Tethys: implications for the age of radiolarites in the Hellenides. *Bull. Geol. Soc. Greece* XXVIII/3, 13–23.

Belak M., Pamić J., Kolar-Jurkovšek T., Pécskay Z. & Karan D. 1995: Alpine regional metamorphic complex of Mt. Medvednica (northwestern Croatia). In: Vlahović I., Velić I. & Šparica M. (Eds.): Proceedings of the 1st Croatian Geological Congress, Opatija, 18–21.10.1995. *Inst. Geol.,* Zagreb, 1, 67–70 (in Croatian).

Bonatti E. & Michael P.J. 1989: Mantle peridotites from continental rifts to ocean basins to subduction zones. *Earth. Planet. Sci. Lett.* 91, 297–311.

Brey G.P. & Köhler T. 1990: Geothermobarometry in four-phase lherzolites II. New thermobarometers, and practical assessment of existing thermobarometers. *J. Petrology* 31, 1353–1378.

Coleman R.G. 1977: Ophiolites. *Springer Verlag*, New York, 1–229.

Conrad W.K. & Kay R.W. 1984: Ultramafic and mafic inclusions from Adak Islands: Crystallization history, and implications for the nature of primary magmas and crustal evolution in the Aleutian arc. *J. Petrology* 25, 88–125.

Crnković B. 1960: The hornblende-peridotite on the north side of Medvednica-Zagrebačka gora Mountain. *Geol. Vjesnik* 13, 57–64 (in Croatian, English summary).

Crnković B. 1963: Petrography and petrogenesis of the magmatites of the northern part of Medvednica Mountain. *Geol. Vjesnik* 16, 63–160 (in Croatian, English summary).

DeBari S.M. & Coleman R.G. 1989: Examination of the deep levels of an island arc: Evidence from the Tonsina ultramafic-mafic assemblage, Tonsina, Alaska. *J. Geophys. Res.* 94, 4373–4391.

Dick H.J.B. & Bullen T. 1984: Chromian spinel as a petrogenetic indicator in abisal and alpine-type peridotites and spatially associated lavas. *Contr. Mineral. Petrology* 86, 54–76.

Dimitrijević M.D. 1983: Geology of Eastern Yugoslavia: a short review. Guide-book, Field Meeting International Working Group IGCP Project 5, Correlation of Pre-variscan and Variscan events in the Alpine-Mediterranean Mountain Belt in Yugoslavia, Yugoslavian Comm. *IGCP,* 1–65.

Downes H., Pantó Gy., Árkai P. & Thirlwall M.F. 1990: Petrology and geochemistry of Mesozoic igneous rock, Bükk Mountains. *Lithos* 24, 201–215.

Evensen N.M., Hamilton P.J. & O'Nions R.K. 1978: Rare earth abundances in chondritic meteorites. *Geochim. Cosmochim. Acta* 42, 1199–1212.

Fabriés J. 1979: Spinel-olivine geothermometry in peridotites from ultramafic complexes. *Contr. Mineral. Petrology* 69, 329–336.

Faryad S.W., Spišiak J., Horvát P., Hovorka D., Dianiška I. & Józsa S. 2005: Petrological and geochemical features of the Meliata mafic rocks from the sutured Triassic oceanic basin, Western Carpathians. *Ofioliti* 30, 27–35.

Goričan S., Halamić J., Grgasović T. & Kolar-Jurkovšek T. 2005: Stratigraphic evolution of Triassic arc-back-arc system in northwestern Croatia. *Bull. Soc. Géol. France* 176, 3–22.

Haas J. & Kovács S. 2001: The Dinaridic-Alpine connection — as seen from Hungary. *Acta Geol. Hung.* 44, 345–362.

Haas J., Mioč P., Pamić J., Tomljenović B., Árkai P., Berczi-Makk A., Koroknai B., Kovács S. & Felgenhauer E. 2000: Complex structural pattern of the Alpine-Dinaridic-Pannonian triple junction. *Int. J. Earth Sci.* 89, 377–389.

Halamić J. 1998: Lithostratigraphic characterisation of Jurassic and Cretaceous sediments with ophiolites at Mts Medvednica, Kalnik and Ivanščica. *Ph.D., Univ. Zagreb,* 1–188 (in Croatian, English summary).

Halamić J. & Goričan Š. 1995: Triasic and Jurassic radiolarites from the Mts. Medvednica and Kalnik. *Geol. Croatica* 48, 129–146.

Halamić J., Slovenec D. & Kolar-Jurkovšek T. 1998: Triassic pelagic limestones in pillow lavas in the Orešje quarry near Gornja Bistra, Medvednica Mt. (Northwest Croatia). *Geol. Croatica* 51, 33–45.

Halamić J., Goričan Š., Slovenec Da. & Kolar-Jurkovšek T. 1999: A Middle Jurassic radiolarite-clastic succession from the Medvednica Mt. (NW Croatia). *Geol. Croatica* 52, 29–57.

Harris R.A. 1995: Geochemistry and tectonomagmatic affinity of the Misgeguk massif, Brooks range ophiolite, Alaska. *Lithos* 35, 1–25.

Harangi Sz., Szabó Cs., Józsa S., Szoldán Zs., Árva-Sós E., Balla M. & Kubovics I. 1996: Mesozoic igneous suites in Hungary: Implications for genesis and tectonic setting in the northwestern part of Tethys. *Int. Geol. Rev.* 38, 336–360.

Harte B. 1976: Rock nomenclature with particular relation to deformation and recrystallization textures in olivine-bearing xenoliths. *J. Geol.* 85, 279–288.

Herak M. 1999: Tectonic interrelation of the Dinarides and the Southern Alps. *Geol. Croatica* 52, 83–98.

Hébert R. & Laurent R. 1990: Mineral chemistry of the plutonic section of the Troodos ophiolite: new constraints for genesis of arc-related ophiolites. In: Malpas J., Moores E., Panayiotou A. & Xenophontos C. (Eds.): Ophiolites–Oceanic Crustal analogues. *Proceedings of Troodos Ophiolite Symposium. Geol. Surv. Department*, Cyprus, 149–163.

Hofmann A.W. 1988: Chemical differentation of the Earth: the relationship between mantle, continental crust, and oceanic crust. *Earth Planet. Sci. Lett.* 90, 297–314.

Hovorka D., Jaroš J., Kratochvíl M., Reichwalder P., Rojkovič I., Spišiak J. & Turanová L. 1985: Ultramafic rocks of the Western Carpathians, Czechoslovakia. *Geol. Inst. Dionýz Štúr*, Bratislava, 1–258.

Huot F. & Maury R.C. 2002: The Round Mountain serpentinite mélange, northern Coast Ranges of California: An association of backarc and arc-related tectonic units. *GSA Bull.* 114, 109–123.

Józsa S. 1999: Petrological and geochemical investigations of the oceanic crust-related magmatic rocks of Darno Hill. *Ph.D. Thesis, Univ. Budapest*, 1–173 (in Hungarian, English summary).

Kamenetsky V.S., Crawford A.J. & Meffre S. 2001: Factors controlling chemistry of magmatic spinel: an empirical study of associated olivine, Cr-spinel and melt inclusions from primitive rocks. *J. Petrology* 42, 655–671.

Karamata S. 1979: The transitional zone between tectonite ultramafic rocks and igneous cumulate rocks in the ophiolite complexes of Yugoslavia. *Bull. SANU* 66, 57–62.

Karamata S., Majer V. & Pamić J. 1980: Ophiolites of Yugoslavia. In: Rocci G. (Ed.): Tethyan Ophiolites. *Ofioliti, Spec. Issue* 1, 105–125.

Karamata S., Olujić J., Protić L., Milovanović D., Vujnović L., Popević A., Memović E., Radovanović Z. & Resimić-Šarić K. 2000: The western belt of the Vardar Zone — the remnant of a marginal sea. In: Karamata S. & Janković S. (Eds.): International Symposium Geology and Metallogeny of the Dinarides and the Vardar zone. *The Academy of Sciences and Arts of the Republic of Srpska,* Banja Luka, Sarajevo, 131–135.

Kepezhinskas P.K., Taylor R.N. & Tanaka H. 1993: Geochemistry of plutonic spinels from the North Kamchatka Arc: comparison with spinels from other tectonic settings. *Mineral. Mag.* 57, 575–589.

Kišpatić M. 1918: Die Eruptivgesteine und kristallinische Schiefer des Agramer Gebirges. *Glasn. Hrv. Prir. Druš.* 30, 1–23.

Kocak K., Isık F., Arslan M. & Zedef V. 2005: Petrological and source region characteristics of ophiolitic hornblende gabbros from the Aksaray and Kayseri regions, central Anatolian crystalline complex, Turkey. *J. Asian Earth Sci.* 25, 883–891.

Koepke J. & Seidel E. 2004: Hornblendites within ophiolites of Crete, Greece: evidence for amphibole-rich cumulates derived from an iron-rich tholeiitic melt. *Ofioliti* 29, 159–175.

Kubovics I. 1984: On the petrogenesis of the north Hungarian basic-ultrabasic magmatic rocks. *Acta Geol. Hung.* 27, 163–189.

Kubovics I. & Bilik I. 1984: Comparative investigation of the Hungarian Mesozoic basic-ultrabasic and some ophiolitic magmatic rocks in the Alp-Carpathian chain. *Acta Geol. Hung.* 27, 321–339.

Leake B.E. & group of authors 1997: Nomenclature of amphiboles. *Eur. J. Mineral.* 9, 623–651.

Leblanc M., Dupuy C. & Merlet C. 1984: Nickel content of olivine as a discriminatory factor between tectonite and cumulate peridotite in ophiolites. *Sci. Géol. Bull.* 37, 131–135.

Lindsley D.H. 1983: Pyroxene thermometry. *Amer. Mineralogist* 68, 477–493.

Lugović B. 1986: Gabbro-peridotite rock association from the northwestern flanks of Mt. Maljen ophiolite massif. *Ph.D. Thesis, Univ. Zagreb*, 1–207 (in Croatian).

Lugović B. & Slovenec Da. 2004: Mantle harzburgites (serpentinites) from Gornje Orešje (Medvednica Mts., Croatia). In: Halamić J. (Ed.): Excursion Guide, Joint Meeting of Croatian and Hungarian Geological Societies on Geology of the Zagorje-Mid-Transdanubian Zone. *Inst. Geol.*, Zagreb, 40–45.

Lugović B., Altherr R., Raczek I., Hofmann A.W. & Majer V. 1991: Geochemistry of peridotites and mafic igneous rocks from the Central Dinaric Ophiolite Belt, Yugoslavia. *Contr. Mineral. Petrology* 106, 201–216.

Lugović B., Šegvić B. & Altherr R. 2006: Petrology and tectonic significance of greenschists from the Medvednica Mts. (Sava unit, NW Croatia). *Ofioliti* 31, 39–50.

Mahéo G., Bertrand H., Guillot S., Villa I.M., Francine Keller F. & Capiez P. 2004: The South Ladakh ophiolites (NW Himalaya, India): an intra-oceanic tholeiitic arc origin with implication for the closure of the Neo-Tethys. *Chem. Geol.* 203, 273–303.

Majer V. 1993: Ophiolite complex of the Banija and Pokuplje region in Croatia and Mt. Pastirevo in northwestern Bosnia. *Acta Geol. HAZU* 23, 39–84 (in Croatian, English summary).

Maksimović Z. & Kolomejceva-Jovanović L. 1987: Composition of coexisting minerals of Yugoslav peridotites and the problems of geothermometry and geobarometry of two ultramafic zones. *Glas SANU, Odel. Prirod.-Matemat. Nauka* 51, 21–52.

Maksimović Z. & Majer V. 1981: Accesory spinels of two main zones of Alpine ultramafic rocks in Yugoslavia. *Bull. Acad. Sci. Serbe, Sci. Naturell.* 21, 47–58.

Moores E.M. & Jackson E.D. 1974: Ophiolites and oceanic crust. *Nature* 250, 136–139.

Morimoto N. 1988: Nomenclature of pyroxenes. *Schweiz. Mineral. Petrogr. Mitt.* 68, 95–111.

Nicolas A. & Jackson E.D. 1972: Répartition en deux provinces des péridotites des chaînes alpines longeant la méditerranée: implications géotectoniques. *Bull. Swiss. Miner. Petrology* 53, 385–401.

Ohara Y. & Ishii T. 1998: Peridotites from southern Mariana forearc: Heterogeneous fluid supply in mantle wedge. *Island Arc* 7, 541–558.

Ohara Y., Kasuga S. & Ishii T. 1996: Peridotites from the Parece Vela Rift in the Pilippine Sea. Upper mantle material exposed in a extinct back-arc basin. *Proc. Japan. Acad.* 72B, 118–123.

Ohara Y., Stern R.J., Ishii T., Yurimoto H. & Yamazaki T. 2002: Peridotites from the Mariana Trough: first look at the mantle beneath an active back-arc. *Contr. Mineral. Petrology* 143, 1–18.

Okrusch M., Sidel E., Kreuzer H. & Harre W. 1978: Jurassic age of metamorphism at the base of the Brezovica peridotite (Yugoslavia). *Earth. Planet. Sci. Lett.* 39, 291–297.

Olker B., Altherr R. & Lugović B. 2001: Metamorphic evolution of mafic granulites from the metamorphic sole of Central Dinaric Ophiolites (Bosnia-Herzegovina). *Abstracts EUG XI Meeting*, 8–12 April 2001, Strasbourg, France, 320–321.

Ozawa K. 1983: Evaluation of olivine-spinel geothermometry as an indicator of thermal history of peridotites. *Contr. Mineral. Petrol*ogy 82, 52–65.

Pamić J.J. 1974: Alpine-type gabbros within the Krivaja-Konjuh ultramafic massif in the Ophiolite Zone of the Dinarides, Yugoslavia. *Tschermaks Min. Petr. Mitt.* 21, 261–279.

Pamić J. 1983: Considerations on the boundary between lherzolite and harzburgite subprovinces in the Dinarides and northern Hellenides. *Ofioliti* 8, 153–164.

Pamić J. 1997: The northwesternmost outcrops of the Dinaridic ophiolites: a case study of Mt. Kalnik (North Croatia). *Acta Geol. Hung.* 40, 37–56.

Pamić J. 2002: The Vardar Zone of the Dinarides and Hellenides versus the Vardar Ocean. *Eclogae Geol. Helv.* 95, 99–113.

Pamić J. 2003: The allochthonous fragments of the Internal Dinaridic units in the western part of the South Pannonian Basin. *Acta Geol. Hung.* 46, 41–62.

Pamić J. & Desmons J. 1989: A complete ophiolite sequence in Rzav, area of Zlatibor and Varda ultramafic massifs, the Dinaride ophiolite zone. *Ofioliti* 14, 13–32.

Pamić J. & Tomljenović B. 1998: Basic geologic data from the Croatian part of the Zagorje-Mid-Transdanubian Zone. *Acta Geol. Hung.* 41, 389–400.

Pamić J., Tomljenović B. & Balen D. 2002: Geodynamic and petrogenetic evolution of Alpine ophiolites from the central and NW Dinarides: an overview. *Lithos* 65, 113–142.

Pandžić J. 1982: Tertiary base of the Northern Croatia and the neighbouring areas. *10. Jub. Kongr. Geol. Jugoslavije* 1, 73–85.

Parkinson I.J. & Pearce J.A. 1998: Peridotites from the Izu-Bonin-Mariana Forearc (ODP Leg 125): evidence for mantle melting and melt-mantle interaction in a supra-subduction zone setting. *J. Petrology* 39, 1577–1618.

Parkinson I.J., Pearce J.A., Thirlwall M.F., Johnson K.T.M. & Ingram G. 1992: Trace element geochemistry of peridotites from the Izu–Bonin–Mariana forearc, Leg 125. *Proc. Ocean Drill. Program Sci. Results* 125, 487–506.

Parlak O., Delaloye M. & Bíngöl E. 1996: Mineral chemistry of ultramafic and mafic cumulates as an indicator of the arc-related origin of the Mersín ophiolite (southern Turkey). *Geol. Rdsch.* 85, 647–661.

Parlak O., Höck V. & Delaloye M. 2002: The suprasubduction zone Poznati-Kersanti ophiolite, southern Turkey: evidence for high-pressure crystal fractionation of ultramafic cumulates. *Lithos* 65, 205–224.

Pearce J.A., Barker P.F., Edwards S.J., Parkinson I.J. & Leat P.T. 2000: Geochemistry and tectonic significance of peridotites from the South Sandwich arc-basin system, South Atlantic. *Contr. Mineral. Petrology* 139, 36–53.

Poljak J. 1942: Ein Beitrag zur Geologie des Kalnik-Gebirges. *Vjes. Hrv. Drž. Geol. Zav. Hrv. Drž. Geol. Muz.* 1, 53–92.

Pouchou J.L. & Pichoir F. 1984: A new model for quantitative analyses. I. Application to the analysis of homogeneous samples. *La Recherche Aérospatiale* 3, 13–38.

Pouchou J.L. & Pichoir F. 1985: "PAP" (ϕ-ρ-Z) correction procedure for improved quantitative microanalysis. In: Armstrong J.T. (Ed.): Microbeam analysis. *San Francisco Press*, 104–106.

Réti Z. 1987: Comparison of the Mesozoic mafic and ultramafic complexes in northern Hungary. *Ofioliti* 12, 43–52.

Robertson A.H.F. & Karamata S. 1994: The role of subduction–accretion processes in the tectonic evolution of the Mesozoic Tethys in Serbia. *Tectonophysics* 234, 73–94.

Roeder P.L. & Emslie R.F. 1970: Olivine-liquid equilibrium. *Contr. Mineral. Petrology* 29, 275–289.

Slovenec Da. 1998: Ophiolitic rocks in the area of the Bistra creek on the northern slopes of Medvednica Mt. *B.Sc. Thesis, Univ. Zagreb*, 1–104 (in Croatian, English summary).

Slovenec Da. 2003: Petrology and geochemistry of the ophiolitic rocks from Medvednica Mt. *Ph.D. Thesis*, *Univ. Zagreb*, 1–180 (in Croatian, English summary).

Slovenec Da. & Lugović B. 2000: Ultramafic cumulate rocks from the Medvednica Mts. ophiolite complex (Northwestern Croatia). In: Vlahović I. & Biondić R. (Eds.): Proceedings of the 2nd Croatian Geological Congress, Cavtat-Dubrovnik, 17–20.5.2000. *Inst. Geol.*, Zagreb, 379–385 (in Croatian, English summary).

Smith A.G. & Spray J.G. 1984: A half-ridge transform model for the Hellenic-Dinaric ophiolites. In: Dixon J.E. & Robertson A.H.F. (Eds.): The geological evolution of the Eastern Mediterranean. *Geol. Soc. London, Spec. Publ.* 17, 629–644.

Stampfli G.M. & Borel G.D. 2002: A plate tectonic model for the Paleozoic and Mesozoic constrained by dynamic plate boundaries and restored synthetic oceanic isochrons. *Earth Planet. Sci. Lett.* 196, 17–33.

Streckeisen A.L. 1974: Classification and nomenclature of plutonic rocks. Recommendations of the IUGS subcommission on the systematics of igneous rocks. *Geol. Rdsch.* 63, 773–786.

Šegvić B., Lugović B. & Ignjatić S. 2005: Petrochemical and geotectonic characteristics of amphibolites from the Zagorje-Mid-Transdanubian shear zone (Mt. Kalnik, Croatia). In: Vlahović I. & Biondić R. (Eds.): 3rd Croatian Geological Congress, Opatija, 29.09.–01.10.2005. *Abstract Book, Croat. Geol. Survey*, Zagreb, 143–144.

Šimunić A. & Pamić J. 1989: Ultramafic rocks from the neighbourhood of Gornje Orešje on the nortwestern flanks of Mt. Medvednica (northern Croatia). *Geol. Vjesnik* 42, 93–101.

Šimunić An., Pikija M., Hećimović I. & Šimunić Al. 1981: Basic geological map 1:100,000. Sheet Varaždin, explanatory notes. *Inst. Geol. Istraž., Zagreb–Sav. Geol. zavod Beograd,* 1–74 (in Croatian).

Šimunić An., Pikija M., Hećimović I. & Šimunić Al. 1982: Basic geological map, 1:100,000. Sheet Varaždin. *Inst. Geol. Istraž., Zagreb–Sav. Geol. zavod Beograd.*

Tomljenović B. 2002: Structural characteristics of Medvednica and Samoborska Gora Mts. *Ph.D. Thesis, Univ. Zagreb*, 1–206 (in Croatian, English summary).

Tribuzio R., Tiepolo M. & Thirlwall M.F. 2000: Origin of titanian pargasite in gabbroic rocks from the Northern Apennine ophiolites (Italy): insights into the late-magmatic evolution of a MOR-type intrusive sequence. *Earth Planet. Sci. Lett.* 176, 281–293.

Trubelja F., Marchig V., Burgath K.P. & Vujović Ž. 1995: Origin of the Jurassic Tethyan ophiolites in Bosnia: a geochemical approach to tectonic setting. *Geol. Croatica* 48, 49–66.

Vragović M. & Marci V. 1973: Carbonate serpentinite from drilling-holes near Lepavina. *Geol. Vjesnik* 26,159–167.

Wells P.R.A. 1977: Pyroxene thermometry in simple and complex systems. *Contr. Mineral. Petrology* 62, 129–139.